A one-sided adaptive truncated exponentially weighted moving average scheme for time between events

Fupeng Xie, Philippe Castagliola, Jinsheng Sun, Anan Tang, Xuelong Hu

A one-sided adaptive truncated exponentially weighted moving average scheme for time between events

FuPeng Xie[a], Philippe Castagliola[b], JinSheng Sun[a], AnAn Tang[c], XueLong Hu[c,*]

[a]*School of Automation, Nanjing University of Science and Technology, Nanjing, China*
[b]*Université de Nantes & LS2N UMR CNRS 6004, Nantes, France*
[c]*School of Management , Nanjing University of Posts and Telecommunications, Nanjing, China*

Abstract

In order to provide a balanced protection against a range of shift sizes in high-quality processes, a new one-sided adaptive truncated exponentially weighted moving average (ATEWMA) control chart with known and estimated parameters is developed for monitoring time-between-events (TBE) data. A dedicated Markov chain model is established for evaluating the run length properties in known and estimated parameters operating conditions. Furthermore, a two-stage optimal design procedure of the proposed scheme is developed based on the average run length (ARL) criteria. Simulation results show that the one-sided ATEWMA TBE scheme with known parameters is superior to its competitors in detecting both upward and downward shifts. Finally, two real data applications are employed to show the implementation of the recommended scheme in the monitoring of TBE data.

*Corresponding Author
Email addresses: xfp@njust.edu.cn (FuPeng Xie), philippe.castagliola@univ-nantes.fr (Philippe Castagliola), jssun67@163.com (JinSheng Sun), tanganan2@sina.com (AnAn Tang), hxl0419@hotmail.com (XueLong Hu)

Keywords: Adaptive truncated EWMA chart; Average run length; Markov chain model; Parameter estimation; Time-between-events;

1. Introduction

As one of the most influential tools in statistical process monitoring (SPM), control charts have been extensively used in various fields, for example, manufacturing industry (see Chong et al. (2021)) and network monitoring (see Perry (2020)). According to Castagliola et al. (2019), in SPM, there are two categories of control charts: the memoryless-type charts (for instance, the Shewhart charts) and the memory-type charts (such as the exponentially weighted moving average (EWMA) charts). Shewhart-type charts are easy to implement and efficient in detecting large shifts, but the fact that they only use the current sample information makes them insensitive to detect small to moderate shifts. As alternatives to Shewhart-type charts, the memory-type charts are more sensitive to detect small to moderate shifts, because they are designed to take both the past and the current information into account. This makes the memory-type charts involve more advantages that motivate more interesting research works.

The conventional control charts are known to be designed for a particular shift level. But, in practice, the potential shift size of the process is rarely know in advance. In this context, Capizzi & Masarotto (2003) designed a new adaptive EWMA (AEWMA) control chart for detecting both small and large mean shifts

simultaneously. In the construction of the AEWMA charting statistic, a suitable function of the current error is used to dynamically weight the current and the past observations, which makes the AEWMA chart in Capizzi & Masarotto (2003) be a smooth combination of a Shewhart chart and an EWMA chart. As mentioned by Psarakis (2015), AEWMA type schemes for normally distributed data have been extensively investigated by researchers, see, for instance, Mitra et al. (2019), Haq & Khoo (2019), and Tang et al. (2019b). Without a doubt, AEWMA type schemes are better choices that can achieve a reasonable balance for both small and large mean shifts. However, most of them introduced above are two-sided schemes. As pointed out by Chiu & Tsai (2013), the traditional two-sided schemes may spend more time on generating an out-of-control signal when a shift in the process parameter occurs. Conversely, one-sided schemes are more appropriate for monitoring processes if the direction of the shift can be anticipated, or when the investigator is only interested in a particular directional shift. For example, information on the increase in the infection rate of a particular disease (such as the COVID-19) is very important for a government to adjust epidemic prevention and to take control measures. Although numerous studies have shown that one-sided schemes have wide potential applications in practice, see, for instance, Wang et al. (2019), Qiao et al. (2020 in press), and Haq (2020), there are few studies on one-sided schemes with an adaptive feature. This fact means that the design of a one-sided adaptive type scheme is a topic of interest.

With the improvement of manufacturing capacity, the occurrence rate of de-

fects (or nonconformities) can be maintained at a very low level, say, parts per million (ppm). These processes are usually named "high-quality processes". The traditional attribute control charts (such as p chart or np chart) are no longer valid for monitoring such processes. In this context, time-between-events (TBE) schemes have been developed to overcome the limits of using traditional attribute charts. A common assumption for high-quality processes is that the occurrence of events (i.e., defects, or nonconformities) can be modeled as a homogeneous Poisson process, for which the time between two consecutive events follows an exponential distribution. Extensive research works and extensions of TBE type schemes based on the geometric, negative binomial, exponential, Gamma, and Weibull distributions have since evolved, see, for example, Urbieta et al. (2017), Xie et al. (2021 in press), Ali & Pievatolo (2016), and Sanusi et al. (2020). Among all available distributions, the exponential one is considered as very suitable for modelling high-quality processes and TBE data. This distribution is not only widely employed in the field of reliability engineering as a model of the time to failure of a component or a system (see Montgomery (2012)), but also potentially be applied to other systems or areas. For instance, in the waiting time modelling (see Xie et al. (2010)), in the monitoring of workplace accidents (see Zhang et al. (2006)), in human health surveillance and monitoring (see Aslam et al. (2014)), and even in earthquake analysis (see Santiago & Smith (2013)). All these applications show that the design of TBE control charts based on the exponential distribution is necessary.

An essential assumption for the design of control charts is that the process parameters are assumed known. But, in real applications, the process parameters are usually unknown. This fact means that the parameters of the process should be estimated before the process monitoring starts. Numerous researches on parameter estimations have been conducted on control charts over these years, see, for instance, Zwetsloot & Woodall (2017), Testik et al. (2020), and Jardim et al. (2020). It is worth noting that, the process parameters used to determine the control limits in Phase II usually need to be estimated from a limited number of Phase I observations. According to Tang et al. (2019a), using the control limit obtained from the known parameter case leads to a deteriorated performance for the scheme with estimated parameters. One effective way is to increase the number of Phase I observations. However, in practice, practitioners cannot wait long to collect such a large amount of Phase I observations, especially in the case of high-quality processes. Meanwhile, a shift may also occur in the process parameter when collecting these Phase I observations. Therefore, an attractive alternative suggested by Mahmoud & Maravelakis (2010) is to adjust the corresponding control limit of the scheme, so that it can provide an effective detection ability for the specified shift that occurs in the process parameter.

In this study, a new one-sided AEWMA scheme using the truncation method is developed for monitoring exponentially distributed TBE data assuming a known shift direction (hereafter named as the one-sided ATEWMA TBE scheme). The main contributions of this paper can be summarized as follows: (1) proposing a

new one-sided ATEWMA TBE scheme in the case of known and estimated parameters, (2) establishing a dedicated Markov chain model for run length (RL) evaluation, and (3) developing an ARL-based optimal design procedure to provide a balanced protection against a range of shift sizes. The outline of this paper is organized as follows: In Section 2, a new one-sided ATEWMA TBE scheme with known and estimated parameters is developed. Subsequently, a dedicated Markov chain model is established in Section 3 to evaluate the RL properties of the recommended scheme. In Section 4, an ARL-based optimal design procedure is developed for detecting both small and large shifts simultaneously. In Section 5, numerical comparisons are performed with two comparative schemes for the detection of both upward and downward mean shifts. Some guidelines concerning the construction of the proposed scheme are also provided. Furthermore, two real data applications are employed in Section 6 to illustrate the implementation of the one-sided ATEWMA TBE scheme in OLED failure time monitoring and aircraft reliability monitoring, respectively. Finally, Section 7 concludes with some remarks and directions for future researches.

2. The proposed one-sided ATEWMA TBE scheme

Let us assumed that the TBE random variable X_t, $t = 1, 2, \ldots$, used in a high-quality process follows an exponential distribution with scale parameter θ, i.e., $X_t \sim \exp(\theta)$. In what follows, a new one-sided ATEWMA TBE scheme is developed in the case of known and estimated parameters to detect both small and large shifts simultaneously.

2.1. The process parameters are known

For the known parameter case, let us assume that θ_0 is the known in-control scale parameter (or mean) of the process. In order to simplify the design of the one-sided ATEWMA TBE scheme with known parameters, a scaled TBE random variable M_t is defined as follows:

$$M_t = \frac{X_t}{\theta_0} = \frac{\theta_1}{\theta_0} \cdot \frac{X_t}{\theta_1}, \tag{1}$$

where θ_1 is the out-of-control scale parameter (or mean) of the exponential distribution. For simplicity, let $\tau = \theta_1/\theta_0$ and $\Theta_t = X_t/\theta_1$, then the scaled TBE random variable M_t in (1) can be restated as:

$$M_t = \tau \cdot \Theta_t, \tag{2}$$

where τ represents the shift level that occurs in the in-control scale parameter θ_0, and Θ_t is a standard exponentially distributed random variable with mean equals to 1. The case $\tau = 1$ denotes that no shift occurs in the scale parameter θ_0, and the process is deemed to be in-control. Otherwise, the case $\tau > 1$ (or $0 < \tau < 1$) means that an upward (or a downward) shift occurs in the scale parameter θ_0.

The truncation method developed by Shu et al. (2007) is adopted for the proposed scheme for the effective detection of upward (or downward) shifts. Taking the one-sided ATEWMA TBE scheme for monitoring upward shifts (hereafter named as the upper-sided ATEWMA TBE scheme) as an example, the idea of

the truncation method used in the upper-sided ATEWMA TBE scheme can be described as follows: at sampling point t, we reset the TBE observation X_t to the value of θ_0 when X_t falls below the in-control mean θ_0. Otherwise, if the TBE observation X_t is larger than the in-control mean value θ_0, the original value of X_t is retained. This new "resetting rule" makes the proposed scheme more sensitive for the process monitoring, as it keeps the shift information in the direction of interest. Without loss of generality, two truncated TBE random variables can be defined to describe the truncation method used in this paper, namely,

- the upper-truncated TBE random variable: $X_t^+ = \max(\theta_0, X_t)$,
- the lower-truncated TBE random variable: $X_t^- = \min(\theta_0, X_t)$.

Based on the scaled TBE random variable M_t defined in (1), both the upper-truncated and the lower-truncated TBE random variables can be restated as:

$$M_t^+ = \max(1, M_t), \tag{3}$$

$$M_t^- = \min(1, M_t). \tag{4}$$

When $\tau = 1$, the in-control mean values of the upper-truncated and lower-truncated TBE random variables M_t^+ and M_t^- are $E(M_t^+) = 1+e^{-1}$ and $E(M_t^-) = 1-e^{-1}$, respectively (see Appendix A in Xie et al. (2021 in press) for details). To further simplify the design of the one-sided ATEWMA TBE chart, the scaling of the upper-truncated and lower-truncated TBE random variables M_t^+ and M_t^- are de-

fined, say,

$$Z_t^+ = \frac{M_t^+}{E(M_t^+)}, \tag{5}$$

$$Z_t^- = \frac{M_t^-}{E(M_t^-)}. \tag{6}$$

Different from the one-sided REWMA TBE scheme developed in Gan (1998) using a fixed EWMA smoothing parameter λ_R, the proposed upper-sided (or lower-sided) ATEWMA TBE scheme is designed by adjusting its smoothing parameter λ as a function of the prediction error $e_t^+ = Z_t^+ - W_{t-1}^+ \left(e_t^- = Z_t^- - W_{t-1}^-\right)$, where W_{t-1}^+ and W_{t-1}^- are the upper-sided and lower-sided ATEWMA TBE charting statistics at sampling point $t-1$, respectively. Based on this condition, two one-sided ATEWMA TBE schemes for respectively detecting increases and decreases in the in-control scale parameter θ_0 are designed as follows:

- For the upward shift detection, the charting statistic W_t^+ of the upper-sided ATEWMA TBE scheme, at sampling point $t = 1, 2, \ldots$, is defined as,

$$W_t^+ = W_{t-1}^+ + \phi(e_t^+) = \omega(e_t^+) Z_t^+ + \left(1 - \omega(e_t^+)\right) W_{t-1}^+. \tag{7}$$

- Meanwhile, for detecting downward shifts, the charting statistic W_t^- of the lower-sided ATEWMA TBE scheme is defined as,

$$W_t^- = W_{t-1}^- + \phi(e_t^-) = \omega(e_t^-) Z_t^- + \left(1 - \omega(e_t^-)\right) W_{t-1}^-, \tag{8}$$

where $\omega(e_t^+) = \phi(e_t^+)/e_t^+$ and $\omega(e_t^-) = \phi(e_t^-)/e_t^-$ are the weights of the upper-sided and lower-sided ATEWMA TBE charting statistics, respectively. The initial values for W_t^+ and W_t^- are set to $W_0^+ = W_0^- = 1$. Meanwhile, note that $\phi(e_t^+)$ and $\phi(e_t^-)$ are the Huber's score functions defined as follows:

$$\phi(\varepsilon) = \begin{cases} \varepsilon + (1-\lambda) \times k, & \varepsilon < -k \\ \lambda \times \varepsilon, & |\varepsilon| \leqslant k \\ \varepsilon - (1-\lambda) \times k, & \varepsilon > k \end{cases} \tag{9}$$

where $k \geqslant 0$, and $\lambda \in (0, 1]$ is the smoothing parameter of the one-sided ATEWMA TBE scheme. The implementation of Huber's score function makes the suggested one-sided ATEWMA TBE scheme to be a smooth combination of the Shewhart TBE chart and the one-sided EWMA TBE chart using the truncation method. For the upper-sided (or lower-sided) ATEWMA TBE scheme, an out-of-control signal is generated, if W_t^+ (W_t^-) falls above (below) the control limit H^+ (H^-) of the proposed scheme.

2.2. The process parameters are unknown

In real situations, process parameters are rarely known in advance. This fact means that the process parameters need to be estimated from different Phase I TBE observations Y_t, $t = 1, 2, \ldots$. In this paper, the in-control scale parameter (or mean) θ_0 is estimated using ℓ in-control TBE observations collected in Phase I, namely, $Y_1, Y_2, \cdots, Y_\ell$. According to Zhang et al. (2014), the maximum likeli-

hood estimator $\widehat{\theta}_0$ of θ_0 is given as follows:

$$\widehat{\theta}_0 = \frac{1}{\ell}\sum_{t=1}^{\ell} Y_t. \tag{10}$$

Similar to the known parameter case, the scaled TBE random variable $\widehat{M}_t$ with estimated parameter $\widehat{\theta}_0$ can be given as follows:

$$\widehat{M}_t = \frac{X_t}{\widehat{\theta}_0} = \frac{\theta_0}{\widehat{\theta}_0} \cdot \frac{\theta_1}{\theta_0} \cdot \frac{X_t}{\theta_1}. \tag{11}$$

Furthermore, according to Ozsan et al. (2010), let us define $U = \theta_0/\widehat{\theta}_0$, and then the estimated TBE random variable $\widehat{M}_t$ in (11) can be restated as:

$$\widehat{M}_t = U \cdot \tau \cdot \Theta_t, \tag{12}$$

where τ and Θ_t have already been defined in Section 2.1. Additionally, U is a random variable, which represents the ratio of the in-control scale parameter θ_0 to its estimator $\widehat{\theta}_0$. It has been proven that U follows an inverse Gamma distribution (see Ozsan et al. (2010)), and the probability density function (p.d.f.) $f_U(u|\ell)$ of U is defined as follows:

$$f_U(u|\ell) = \frac{\ell^\ell}{(\ell-1)!} u^{-\ell-1} \exp\left(-\frac{\ell}{u}\right). \tag{13}$$

Due to the use of the estimator $\widehat{\theta}_0$ in (10), the corresponding truncated TBE random variables $\widehat{M}_t^+$ and $\widehat{M}_t^-$ with estimated parameters can be, respectively,

written as,

$$\widehat{M}_t^+ = \max(1, \widehat{M}_t), \tag{14}$$

$$\widehat{M}_t^- = \min(1, \widehat{M}_t). \tag{15}$$

The in-control mean values of $\widehat{M}_t^+$ and $\widehat{M}_t^-$ are $E(\widehat{M}_t^+) = 1+Ue^{-\frac{1}{U}}$ and $E(\widehat{M}_t^-) = U - Ue^{-\frac{1}{U}}$, respectively, conditioned on U (see Appendix A in Xie et al. (2021 in press) for details). Similarly, the scaling of the upper-truncated and lower-truncated TBE random variables $\widehat{M}_t^+$ and $\widehat{M}_t^-$ with estimated parameters are given as follows:

$$\widehat{Z}_t^{\,+} = \frac{\widehat{M}_t^+}{E(\widehat{M}_t^+)}, \tag{16}$$

$$\widehat{Z}_t^{\,-} = \frac{\widehat{M}_t^-}{E(\widehat{M}_t^-)}. \tag{17}$$

The upper-sided and lower-sided ATEWMA TBE charting statistics with estimated parameters, at sampling point t, can be written as follows:

$$\widehat{W}_t^+ = \widehat{W}_{t-1}^+ + \phi(\widehat{e}_t^{\,+}) = \omega(\widehat{e}_t^{\,+})\widehat{Z}_t^{\,+} + \left(1 - \omega(\widehat{e}_t^{\,+})\right)\widehat{W}_{t-1}^+, \tag{18}$$

$$\widehat{W}_t^- = \widehat{W}_{t-1}^- + \phi(\widehat{e}_t^{\,-}) = \omega(\widehat{e}_t^{\,-})\widehat{Z}_t^{\,-} + \left(1 - \omega(\widehat{e}_t^{\,-})\right)\widehat{W}_{t-1}^-, \tag{19}$$

where the initial value for $\widehat{W}_t^+$ (or $\widehat{W}_t^-$) is set to $\widehat{W}_0^+ = E(\widehat{Z}_t^{\,+}) = 1$ ($\widehat{W}_0^- = E(\widehat{Z}_t^{\,-}) = 1$), and $\phi(\cdot)$ is the Huber's score function given in (9). The upper-sided (or lower-sided) ATEWMA TBE scheme gives an out-of-control signal when the

charting statistic $\widehat{W}_t^+ > \widehat{H}^+$ ($\widehat{W}_t^- < \widehat{H}^-$), where $\widehat{H}^+$ and $\widehat{H}^-$ are the adjusted control limits of the upper-sided and lower-sided ATEWMA TBE schemes, respectively.

3. Run length evaluation

As one of the most widely used criterion in control charts, the average run length (ARL) is defined as the expected number of charting statistics plotted on the one-sided ATEWMA TBE scheme until an out-of-control signal is generated. Commonly, if there is no shift occurs in the process, a control chart is expected to run with a large in-control ARL value (hereafter denoted as the ARL_0), but when the process is out-of-control, the corresponding out-of-control ARL (hereafter denoted as the ARL_1) value is expected to be as small as possible. In this section, an appropriate discrete-state Markov chain model is established to investigate the ARL performance of the one-sided ATEWMA TBE scheme in the case of known and estimated parameters. Due to the space limitation, only the upper-sided ATEWMA TBE scheme with known and estimated parameters is selected as an example to illustrate the establishment of the Markov chain model. For more details about the Markov chain model of the lower-sided ATEWMA TBE scheme with known and estimated parameters, readers can refer to Appendix A.

3.1. The Markov chain model for the known parameter case

The basic idea of the Markov chain model is to define the transition states by dividing the in-control region into a finite number of sub-intervals, and then to approximate the charting statistic using the mid-point value of each sub-interval. In

this study, we divide the in-control region into m sub-intervals, namely, transient state 1, transient state 2, $\cdots$, transient state m, and then the ARL of the upper-sided ATEWMA TBE scheme with known parameters can be computed using,

$$\mathrm{ARL} = \mathbf{p}^{\mathsf{T}}(\mathbf{I} - \mathbf{Q})^{-1}\mathbf{1}, \tag{20}$$

where $\mathbf{p} = (p_1, p_2, \ldots, p_m)^{\mathsf{T}}$ is the initial probability vector that corresponds to m transient states, and $\mathbf{Q} = [q_{i,j}]_{m\times m}$ is the transition probability matrix. Moreover, $\mathbf{1}$ is an $m \times 1$-dimensional vector of 1's, and $\mathbf{I}$ is an $m \times m$-dimensional identity matrix. It is easy to obtain that the in-control region is $[1/\left(1 + e^{-1}\right), H^{+}]$. Hence, the width Δ^{+} of each sub-interval can be given as,

$$\Delta^{+} = \frac{1}{m}\left(H^{+} - \frac{1}{1 + e^{-1}}\right). \tag{21}$$

For the proposed scheme with known parameters, the charting statistic W_t^{+} is regarded as in "transient state i", when $W_t^{+} \in \left(E_i^{+} - \Delta^{+}/2, E_i^{+} + \Delta^{+}/2\right]$, where $E_i^{+} = 1/\left(1 + e^{-1}\right) + (i - 1/2)\Delta^{+}$ is the mid-point value of the ith sub-interval, $i = 1, 2, \ldots, m$, see Figure 1.

(Please insert Figure 1 here)

As the elements of the transition probability matrix $\mathbf{Q}$, the one-step transient probabilities $q_{i,j}$ from transient state i to transient state j can be computed as

follows:

$$
\begin{aligned}
q_{i,j} &= \Pr\left(W_t^+ \in \text{transient state } j \;\middle|\; W_{t-1}^+ \in \text{transient state } i\right) \\
&= \Pr\left(E_j^+ - \frac{\Delta^+}{2} < W_t^+ \leqslant E_j^+ + \frac{\Delta^+}{2} \middle| W_{t-1}^+ = E_i^+\right) \\
&= \Pr\left(E_j^+ - E_i^+ - \frac{\Delta^+}{2} < \phi(Z_t^+ - W_{t-1}^+) \leqslant E_j^+ - E_i^+ + \frac{\Delta^+}{2}\right)
\end{aligned} \tag{22}
$$

where $i = 1, 2, \ldots, m$, and $j = 1, 2, \ldots, m$. After some algebraic calculations, the one-step transient probabilities $q_{i,j}$ are equivalent to,

$$
\begin{aligned}
q_{i,j} &= \Pr\left(E_i^+ + \phi^{-1}\left(E_j^+ - E_i^+ - \frac{\Delta^+}{2}\right) < Z_t^+ \leqslant E_i^+ + \phi^{-1}\left(E_j^+ - E_i^+ + \frac{\Delta^+}{2}\right)\right) \\
&= \Pr\left(\left(1 + e^{-1}\right)\left[E_i^+ + \phi^{-1}\left(E_j^+ - E_i^+ - \frac{\Delta^+}{2}\right)\right] < M_t^+ \leqslant \left(1 + e^{-1}\right)\right. \\
&\quad \left.\left[E_i^+ + \phi^{-1}\left(E_j^+ - E_i^+ + \frac{\Delta^+}{2}\right)\right]\right)
\end{aligned} \tag{23}
$$

where the Huber's inverse score function $\phi^{-1}(\cdot)$ is given as,

$$
\phi^{-1}(\varepsilon) = \begin{cases} \varepsilon - (1-\lambda) \times k, & \varepsilon < -\lambda \times k \\ \varepsilon/\lambda, & |\varepsilon| \leqslant \lambda \times k \\ \varepsilon + (1-\lambda) \times k. & \varepsilon > \lambda \times k \end{cases} \tag{24}
$$

For simplicity, let us define,

$$\Psi_1 = \left(1 + e^{-1}\right)\left[E_i^+ + \phi^{-1}\left(E_j^+ - E_i^+ - \frac{\Delta^+}{2}\right)\right], \tag{25}$$

$$\Psi_2 = \left(1 + e^{-1}\right)\left[E_i^+ + \phi^{-1}\left(E_j^+ - E_i^+ + \frac{\Delta^+}{2}\right)\right]. \tag{26}$$

Therefore, the one-step transient probabilities $q_{i,j}$ can be computed as follows:

$$q_{i,j} = \begin{cases} 0, & \text{if } \Psi_2 < 1 \\ F_\Theta\left(\dfrac{\Psi_2}{\tau}\right), & \text{if } \Psi_2 \geqslant 1 \text{ and } \Psi_1 < 1 \\ F_\Theta\left(\dfrac{\Psi_2}{\tau}\right) - F_\Theta\left(\dfrac{\Psi_1}{\tau}\right), & \text{if } \Psi_2 \geqslant 1 \text{ and } \Psi_1 \geqslant 1 \end{cases} \tag{27}$$

where $F_\Theta(\cdot)$ is the cumulative distribution function (c.d.f.) of the standard exponentially distributed random variable Θ_t defined in (2). Furthermore, the elements p_j of the initial probability vector $\mathbf{p}$ are defined as follows:

$$p_j = \begin{cases} 1, & E_j^+ - \dfrac{\Delta^+}{2} < W_0^+ \leqslant E_j^+ + \dfrac{\Delta^+}{2} \\ 0, & \text{otherwise} \end{cases} \tag{28}$$

where $j = 1, 2, \ldots, m$, and $W_0^+ = E(Z_t^+) = 1$.

3.2. The Markov chain model for the estimated parameter case

Unlike the upper-sided ATEWMA TBE scheme with known parameters, the unconditional ARL value (hereafter denoted as $\widehat{\mathrm{ARL}}$) for the parameter estimation case can be computed by integrating the $\widehat{\mathrm{ARL}}(\tau|u)$ (i.e., the conditional ARL

value) with respect to u, i.e.,

$$\widehat{\mathrm{ARL}} = \int_0^{+\infty} \widehat{\mathrm{ARL}}(\tau|u) \times f_U(u|\ell)\, \mathrm{d}u, \tag{29}$$

where

$$\widehat{\mathrm{ARL}}(\tau|u) = \widehat{\mathbf{p}}^{\mathsf{T}}(\mathbf{I} - \widehat{\mathbf{Q}})^{-1}\mathbf{1}, \tag{30}$$

and $f_U(u|\ell)$ is the p.d.f. of the random variable U defined in (13). Note that $\widehat{\mathbf{p}} = (\widehat{p}_1, \widehat{p}_2, \cdots, \widehat{p}_m)^{\mathsf{T}}$ is an $m \times 1$-dimensional initial probability vector with estimated parameters, and $\widehat{\mathbf{Q}}$ contains the corresponding transient probabilities $\widehat{q}_{i,j}$ of going from transient state i to transient state j. The establishment of the Markov chain model for the estimated parameter case is similar to that one for the known parameter case, where the one-step transient probabilities $\widehat{q}_{i,j}$ in the estimated parameter case are given as:

$$\begin{aligned}
\widehat{q}_{i,j} &= \Pr\left(\widehat{W}_t^+ \in \text{transient state } j \mid \widehat{W}_{t-1}^+ \in \text{transient state } i\right) \\
&= \Pr\left(\left(1 + ue^{-\frac{1}{u}}\right)\left[\widehat{E}_i^+ + \phi^{-1}\left(\widehat{E}_j^+ - \widehat{E}_i^+ - \frac{\widehat{\Delta}^+}{2}\right)\right] < \widehat{M}_t^+ \leqslant \left(1 + ue^{-\frac{1}{u}}\right)\right. \\
&\quad \left.\left[\widehat{E}_i^+ + \phi^{-1}\left(\widehat{E}_j^+ - \widehat{E}_i^+ + \frac{\widehat{\Delta}^+}{2}\right)\right]\right)
\end{aligned} \tag{31}$$

Note that $\widehat{E}_j^+ = 1/\left(1 + ue^{-\frac{1}{u}}\right) + (j - 1/2)\widehat{\Delta}^+$ is the mid-point value of the jth sub-interval, and $\widehat{\Delta}^+ = \left(\widehat{H}^+ - 1/\left(1 + ue^{-\frac{1}{u}}\right)\right)/m$ is the width of the jth

sub-interval, where $j = 1, 2, \ldots, m$. Furthermore, if we define,

$$\widehat{\Psi}_1 = \left(1 + ue^{-\frac{1}{u}}\right)\left[\widehat{E}_i^+ + \phi^{-1}\left(\widehat{E}_j^+ - \widehat{E}_i^+ - \frac{\widehat{\Delta}^+}{2}\right)\right], \tag{32}$$

$$\widehat{\Psi}_2 = \left(1 + ue^{-\frac{1}{u}}\right)\left[\widehat{E}_i^+ + \phi^{-1}\left(\widehat{E}_j^+ - \widehat{E}_i^+ + \frac{\widehat{\Delta}^+}{2}\right)\right]. \tag{33}$$

Then, the entire one-step transient probabilities $\widehat{q}_{i,j}$ can be computed using,

$$\widehat{q}_{i,j} = \begin{cases} 0, & \text{if } \widehat{\Psi}_2 < 1 \\ F_\Theta\left(\dfrac{\widehat{\Psi}_2}{u \times \tau}\right), & \text{if } \widehat{\Psi}_2 \geqslant 1 \text{ and } \widehat{\Psi}_1 < 1 \\ F_\Theta\left(\dfrac{\widehat{\Psi}_2}{u \times \tau}\right) - F_\Theta\left(\dfrac{\widehat{\Psi}_1}{u \times \tau}\right), & \text{if } \widehat{\Psi}_2 \geqslant 1 \text{ and } \widehat{\Psi}_1 \geqslant 1 \end{cases} \tag{34}$$

where $i = 1, 2, \ldots, m$, and $j = 1, 2, \ldots, m$. Meanwhile, the elements $\widehat{p}_j$ of the initial probability vector $\widehat{\mathbf{p}}$ are,

$$\widehat{p}_j = \begin{cases} 1, & \widehat{E}_j^+ - \dfrac{\widehat{\Delta}^+}{2} < \widehat{W}_0^+ \leqslant \widehat{E}_j^+ + \dfrac{\widehat{\Delta}^+}{2} \\ 0, & \text{otherwise} \end{cases} \tag{35}$$

where $\widehat{W}_0^+ = E(\widehat{Z}_t^+) = 1$.

Finally, in order to overcome the computational difficulties caused by the evaluation of (29), the Gauss-Legendre quadrature method is considered in this paper to obtain an accurate approximation.

4. Optimal design of the one-sided ATEWMA TBE scheme

The optimal design of the one-sided ATEWMA TBE scheme aims at finding a scheme, which can simultaneously provide the minimum ARL_1 (denoted as $\mathrm{ARL}_{\min}$) value for a specified small shift τ_S and an approximate $\mathrm{ARL}_{\min}$ value for a specified large shift τ_L, among those one-sided ATEWMA TBE schemes leading to the same desired ARL_0 value.

For the proposed one-sided ATEWMA TBE scheme, the combination of the design parameters obtained from the optimal design procedure is named as the optimal parameter combination, and the scheme with the optimal parameter combination is denoted as the optimal one-sided ATEWMA TBE scheme. In this study, a two-stage optimal design procedure, similar to the one presented in Capizzi & Masarotto (2003), is introduced for determining the optimal parameter combination of the one-sided ATEWMA TBE scheme. Due to the space limitation, only the upper-sided ATEWMA TBE scheme with known parameters is selected here for illustration, and the steps are given as follows:

Step 1: Choose a desired ARL_0 value, and two different shift values, i.e., a small mean shift τ_S, and a large mean shift τ_L.

Step 2: With the constraint on the desired ARL_0, search the optimal parameter combination $\gamma^* = \{\lambda_L^*, k_L^*, H_L^{+*}\}$ of the upper-side ATEWMA TBE scheme for the specified large shift τ_L. The corresponding result can be regarded as the solution of the following nonlinear minimization problem,

i.e.,

$$\begin{cases} \gamma^* = \underset{\gamma=\{\lambda_L, k_L, H_L^+\}}{\arg\min} \ \mathrm{ARL}_1(\gamma, \tau_L). \\ \text{Subject to :} \\ \mathrm{ARL}(\gamma^*, \tau_L = 1) = \mathrm{ARL}_0, \end{cases} \tag{36}$$

where the ARL value of the upper-sided ATEWMA TBE scheme with known parameters can be computed using (20).

Step 3: Select a small positive constant α, for example, $\alpha = 0.05$, and then the optimal parameter combination $\zeta^* = \{\lambda^*, k^*, H^{+*}\}$ of the proposed scheme can be searched for detecting both the small shift τ_S and the large shift τ_L using the following equations,

$$\begin{cases} \zeta^* = \underset{\zeta=\{\lambda, k, H^+\}}{\arg\min} \ \mathrm{ARL}_1(\zeta, \tau_S). \\ \text{Subject to :} \\ \mathrm{ARL}(\zeta^*, \tau_S = 1) = \mathrm{ARL}_0, \\ \mathrm{ARL}_1(\zeta^*, \tau_L) \leqslant (1 + \alpha) \times \mathrm{ARL}_1(\gamma^*, \tau_L). \end{cases} \tag{37}$$

More specifically, using equation (37), the upper-sided ATEWMA TBE scheme with optimal parameter combination ζ^* provides the $\mathrm{ARL}_{\min}$ value for the specified small shift τ_S. Meanwhile, the implementation of the positive constant α in (37) ensures that the ARL_1 value of the proposed scheme for the specified large shift τ_L is "nearly minimum".

Considering the computational difficulties in the optimal design procedure, we

suggest the use of an improved particle swarm optimization algorithm, named the DNSPSO algorithm, to solve the nonlinear minimization problem presented in (36) and (37). For more details on the DNSPSO algorithm, readers can refer to Wang et al. (2013).

According to the optimal design procedure described above, for several desired values of $\mathrm{ARL}_0 \in \{200, 370, 500\}$ and different shift combinations (τ_S, τ_L), the optimal parameter combinations ζ^* of the upper-sided and lower-sided ATEWMA TBE schemes with known parameters are listed in Tables 1 and 2, respectively. For instance, when the desired $\mathrm{ARL}_0 = 370$, the optimal parameter combination $\zeta^* = \{\lambda^*, k^*, H^{+*}\}$ of the upper-sided ATEWMA TBE scheme is $\{0.2051, 4.9170, 1.7620\}$ for $(\tau_S, \tau_L) = (1.3, 3)$. Meanwhile, when $(\tau_S, \tau_L) = (0.7, 0.1)$, the corresponding optimal parameter combination $\zeta^* = \{\lambda^*, k^*, H^{-*}\}$ of the lower-sided ATEWMA TBE scheme is $\{0.2951, 2.3076, 0.3983\}$.

(Please insert Tables 1 and 2 here)

As pointed out by Saleh et al. (2013), the parameter estimation has a significant impact on the Phase II performance of the conventional AEWMA scheme. Motivated by this fact, we further study the effect of parameter estimation on the one-sided ATEWMA TBE scheme. Due to the space limitation, only the case of $\mathrm{ARL}_0 = 370$ is considered here for illustration. Similar to the study in Saleh et al. (2013), with the optimal parameter combinations ζ^* determined in the known parameter case, the in-control $\widehat{\mathrm{ARL}}$ (i.e., $\widehat{\mathrm{ARL}_0}$) values of the proposed scheme with estimated parameters are shown in Table 3.

(Please insert Table 3 here)

In order to provide a fair performance comparison between the one-sided ATEWMA TBE scheme with estimated parameters and its known parameter counterpart, both schemes should be designed based on the same in-control ARL value (i.e., $\widehat{\mathrm{ARL}}_0 = \mathrm{ARL}_0$). One effective way to achieve this condition is to adjust the control limits in the estimated parameter case, so that the scheme can provide a desired $\widehat{\mathrm{ARL}}_0$ when various numbers ℓ of TBE observations collected in Phase I are pre-specified. Based on this way, the upper-sided (or lower-sided) ATEWMA TBE scheme with estimated parameters can produce the desired $\widehat{\mathrm{ARL}}_0$ using the design parameter combination $\{\lambda^*, k^*, \widehat{H}^{+*}\}$ (or $\{\lambda^*, k^*, \widehat{H}^{-*}\}$), where λ^* and k^* are those optimal design parameters determined in the known parameter case, and $\widehat{H}^{+*}$ (or $\widehat{H}^{-*}$) is the corresponding adjusted upper (lower) control limit of the proposed scheme with estimated parameters. In this paper, we define the design parameter combinations $\widehat{\zeta}^* = \{\lambda^*, k^*, \widehat{H}^{+*}\}$ and $\widehat{\zeta}^* = \{\lambda^*, k^*, \widehat{H}^{-*}\}$ as the optimal parameter combinations of the upper-sided and lower-sided ATEWMA TBE schemes with estimated parameters, respectively. With the constraint on the desired $\widehat{\mathrm{ARL}}_0 = 370$, the adjusted control limits $\widehat{H}^{+*}$ and $\widehat{H}^{-*}$ of the proposed schemes are given in Table 4 for $\ell \in \{20, 50, 100, 300, 500, 1000\}$.

(Please insert Table 4 here)

From Tables 3 and 4, we can draw the following conclusions:

- As it can be seen from Table 3, for a fixed shift combination (τ_S, τ_L), the difference between ARL_0 (corresponding to the known parameter case, say,

$\ell = +\infty$) and $\widehat{\mathrm{ARL}}_0$ (associated with $\ell \in \{20, 50, 100, 300, 500, 1000\}$) decreases as ℓ increases. That is to say, the effect of the parameter estimation on the $\widehat{\mathrm{ARL}}_0$ is large when ℓ is small.

- Note from Tables 1, 2, and 4 that, for a fixed shift combination (τ_S, τ_L), the adjusted control limits $\widehat{H}^{+*}$ (or $\widehat{H}^{-*}$) of the proposed upper-sided (lower-sided) ATEWMA TBE scheme increases (decreases) as ℓ increases.

It should be stressed that the goal of the study for the parameter estimation case is not to show the superiority of the one-sided ATEWMA TBE scheme over its competitors, but to investigate the impact of the Phase I parameter estimation on the ARL performance of the proposed scheme.

5. Comparative studies

Two comparative schemes are introduced here for comparison with the one-sided ATEWMA TBE scheme in the case of known and estimated parameters: one is the one-sided REWMA TBE scheme designed by Gan (1998), and the other one is the one-sided AEWMA TBE scheme proposed in Hu et al. (2021).

5.1. The one-sided REWMA TBE scheme

The one-sided exponential EWMA chart with reflecting boundaries (i.e., the one-sided REWMA TBE scheme in this paper) was firstly designed by Gan (1998) to monitor either increases or decreases in the process mean.

- For the upper-sided REWMA TBE scheme, its charting statistic is given as:

$$Q_{R,t}^{+} = \max\left(B_U, \lambda_R M_t + (1-\lambda_R) Q_{R,t-1}^{+}\right). \tag{38}$$

- Meanwhile, the monitoring statistic of the lower-sided REWMA TBE scheme is defined as follows:

$$Q_{R,t}^{-} = \min\left(B_L, \lambda_R M_t + (1-\lambda_R) Q_{R,t-1}^{-}\right), \tag{39}$$

where B_U and B_L are the reflecting boundaries of the upper-sided and lower-sided REWMA TBE schemes, respectively. In addition, λ_R represents the smoothing factor, the initial value $Q_{R,0}^{+} = Q_{R,0}^{-} = E(M_t) = 1$, and both B_U and B_L are suggested to be set at 1. Similar to the optimal design procedure designed in Xie et al. (2021 in press), the optimal parameter combination of the one-sided REWMA TBE scheme can be easily obtained for a fixed mean shift τ_R. More specifically, based on $\mathrm{ARL}_0 = \widehat{\mathrm{ARL}}_0 = 370$, the optimal parameter combinations of the one-sided REWMA TBE scheme with known (i.e., $\ell = +\infty$) and estimated (i.e., $\ell = 100$) parameters are presented in Table 5 for different designed shift levels τ_R, where τ_R is a particular shift size for which the one-sided REWMA TBE scheme is optimally designed, λ_R^* is the optimal smoothing factor, h_R^{+*} (or h_R^{-*}) is the control limit of the upper-sided (lower-sided) REWMA TBE scheme with known parameters, and $\widehat{h}_R^{+*}$ (or $\widehat{h}_R^{-*}$) is the adjusted control limit of the upper-sided (lower-sided) REWMA TBE scheme with estimated parameters.

5.2. The one-sided AEWMA TBE scheme

Similar to the methodology used for the one-sided REWMA TBE scheme, the one-sided AEWMA TBE scheme was firstly introduced by Hu et al. (2021) for detecting both small and large shifts simultaneously. As a comparison, the charting statistic of the upper-sided AEWMA TBE scheme is given as:

$$Q_{A,t}^{+} = \max\left(1, \omega(e_{A,t}^{+})M_t + \left(1 - \omega(e_{A,t}^{+})\right) Q_{A,t-1}^{+}\right), \tag{40}$$

where $e_{A,t}^{+} = M_t - Q_{A,t-1}^{+}$, and the weight $\omega(e_{A,t}^{+}) = \phi(e_{A,t}^{+})/e_{A,t}^{+}$. The Huber's score function $\phi(\cdot)$ used in the one-sided AEWMA TBE scheme is the same as it is shown in (11), excepted that λ should be replaced with λ_A, where λ_A is the smoothing parameter of one-sided AEWMA TBE scheme. On the other side, for the lower-sided AEWMA TBE scheme, its charting statistic is defined as follows:

$$Q_{A,t}^{-} = \min\left(1, \omega(e_{A,t}^{-})M_t + \left(1 - \omega(e_{A,t}^{-})\right) Q_{A,t-1}^{-}\right), \tag{41}$$

where the error $e_{A,t}^{-} = M_t - Q_{A,t-1}^{-}$, and $\omega(e_{A,t}^{-}) = \phi(e_{A,t}^{-})/e_{A,t}^{-}$. Additionally, the initial values of this comparative scheme are set to $Q_{A,0}^{+} = Q_{A,0}^{-} = E(M_t) = 1$.

Although an optimal design procedure of the one-sided AEWMA TBE scheme has been introduced by Hu et al. (2021), the corresponding two-stage procedure developed in this paper is also popular and it is adopted for this existing comparative scheme to provide a fair comparison with the proposed one-sided ATEWMA TBE scheme. The optimal parameter combinations of the one-sided AEWMA

TBE chart with known and estimated parameters are presented in Table 5 for $\mathrm{ARL}_0 = \widehat{\mathrm{ARL}}_0 = 370$ and $\ell = 100$, where h_A^{+*} and h_A^{-*} (or $\widehat{h}_A^{+*}$ and $\widehat{h}_A^{-*}$) are the control limits (adjusted control limits) of the upper-sided and lower-sided AEWMA TBE schemes with known (estimated) parameters, respectively.

5.3. Performance comparison

Without loss of generality, with the constraint on the desired ARL_0, the smaller the ARL_1 for the specified shift level τ, the better the performance of the control chart. In this paper, based on $\mathrm{ARL}_0 = 370$ and $m = 151$, the ARL_1 performance of the one-sided ATEWMA TBE scheme in detecting either upward or downward shift is compared with that of two comparative schemes, respectively.

In the case of known parameter, the ARL_1 values of the one-sided ATEWMA TBE scheme and the one-sided AEWMA TBE scheme in detecting both upward and downward shifts τ are presented in Tables 6 and 7, respectively. Note that the optimal parameter combinations of these two schemes for different shift combinations (τ_S, τ_L) are obtained from Tables 1, 2, and 5, respectively. For example, when the desired $\mathrm{ARL}_0 = 370$ and the specified upward shift combination $(\tau_S, \tau_L) = (1.5, 3)$, the ARL_1 values of the upper-sided ATEWMA TBE scheme and the upper-sided AEWMA TBE scheme for the upward shift $\tau = 2$ are 11.46 and 12.13, respectively (see Table 6). Meanwhile, if a downward shift combination $(\tau_S, \tau_L) = (0.7, 0.2)$ is selected, the ARL_1 values of the lower-sided ATEWMA TBE scheme and the lower-sided AEWMA TBE scheme for the down-

ward shift $\tau = 0.8$ are 89.92 and 119.26, respectively (see Table 7).

(Please insert Tables 6 and 7 here)

For the estimated parameter case, the settings in this scenario are similar to the known parameter case, excepted that the number ℓ of in-control TBE observations collected in Phase I need to be fixed first. Taking $\ell = 100$ for illustration, the $\widehat{\mathrm{ARL}}_1$ values of the one-sided ATEWMA TBE scheme and the one-sided AEWMA TBE scheme in detecting both upward and downward shifts τ are presented in Tables 8 and 9, respectively. Meanwhile, the corresponding optimal parameter combinations of these two control charts for $\widehat{\mathrm{ARL}}_0 = 370$ and $\ell = 100$ are shown in Tables 4 and 5, respectively. For instance, when $(\tau_s, \tau_L) = (1.5, 5)$, the optimal parameter combinations of the upper-sided ATEWMA TBE scheme and the upper-sided AEWMA TBE scheme for $\widehat{\mathrm{ARL}}_0 = 370$ and $\ell = 100$ are $\{\lambda^*, k^*, \widehat{H}^{+*}\} = \{0.3105, 7.0272, 2.0854\}$ and $\{\lambda_A^*, k^*, \widehat{h}_A^{+*}\} = \{0.2524, 5.1444, 2.4029\}$, respectively (see Tables 1, 4, and 5). Additionally, the corresponding $\widehat{\mathrm{ARL}}_1$ values of these two schemes for detecting the upward shift $\tau = 1.1$ are 190.19 and 186.10, respectively (see Table 8).

(Please insert Tables 8 and 9 here)

On the other hand, in order to provide some intuitive comparisons between the one-sided ATEWMA TBE scheme and the one-sided REWMA TBE scheme in both the known and the estimated parameter cases, three one-sided REWMA TBE schemes optimally designed for different specified shifts τ_R are selected in this study. The $\ln(\mathrm{ARL}_1)$ and $\ln(\widehat{\mathrm{ARL}}_1)$ curves of these schemes for detecting

both upward and downward shifts τ are given in Figures 2 to 5, respectively. Due to the space limitation, irrespective of the known or the estimated parameter case, the upper-sided ATEWMA TBE scheme is designed based on $\tau_S = 1.5$ and $\tau_L = 4.0$, and the other three different upper-sided REWMA TBE charts are respectively designed to provide the $\mathrm{ARL}_{\min}$ for different specified upward shifts $\tau_R \in \{1.1, 2.5, 5.0\}$. Similarly, in the case of a downward shift detection, the lower-sided ATEWMA TBE scheme is designed for $\tau_S = 0.7$ and $\tau_L = 0.2$, and the other three different lower-sided REWMA TBE charts are designed based on three specified downward shifts $\tau_R \in \{0.9, 0.6, 0.3\}$, respectively.

(Please insert Figures 2 to 5 here)

Based on these comparisons, some conclusions can be drawn as follows:

- For the known parameter case, the one-sided ATEWMA TBE scheme is uniformly more sensitive than the one-sided AEWMA TBE scheme for detecting both upward and downward shifts, especially for small shift ranges. Moreover, in the detection of the upward (downward) shift, the ARL_1 difference between the upper-sided (lower-sided) ATEWMA TBE scheme and the upper-sided (lower-sided) AEWMA TBE scheme decreases, as τ increases (decreases) (see Tables 6 and 7).

- For the estimated parameter case (for instance, $\ell = 100$), most ARL_1 values of the upper-sided AEWMA TBE scheme are smaller than those of the upper-sided ATEWMA TBE scheme. On the contrary, the lower-sided ATEWMA TBE scheme performs better than the lower-sided AEWMA

TBE chart in most downward shift detections. This fact means that the parameter estimation has a significant impact on the ARL performance of these two schemes (see Tables 8 and 9).

- Irrespective of the upward or the downward shift detection case, the adverse effect of parameter estimation on the one-sided ATEWMA TBE chart is relatively smaller than that on the one-sided AEWMA TBE chart. For example, when shift combination $(\tau_S, \tau_L) = (1.1, 3.0)$, the ARL_1 and $\widehat{\mathrm{ARL}}_1$ values of the upper-sided ATEWMA TBE scheme for $\tau = 1.1$ are 176.06 and 175.51, respectively. Meanwhile, the corresponding ARL_1 and $\widehat{\mathrm{ARL}}_1$ values of the upper-sided AEWMA TBE scheme are 182.06 and 170.42, respectively (see Tables 6 and 8).

- No matter in the known or the estimated parameter case, the upper-sided (or lower-sided) ATEWMA TBE scheme can provide an effective protection against both small and large upward (downward) shifts simultaneously. Moreover, the one-sided ATEWMA TBE scheme outperforms the one-sided REWMA TBE scheme over a wide range of shifts, especially for detecting a shift that is much larger or smaller than its designed shift size τ_R. For instance, in the known parameter case, the upper-sided ATEWMA TBE scheme designed for $(\tau_S, \tau_L) = (1.5, 4.0)$ and the upper-sided REWMA TBE chart designed for $\tau_R = 1.1$ have almost the same ARL_1 profiles when the magnitude of upward shift $\tau < 1.5$, but when a large upward shift (for example, $\tau > 2$) occurs in the process, the corresponding upper-sided

ATEWMA TBE scheme can provide a better protection than the upper-sided REWMA TBE scheme designed for $\tau_R = 1.1$ (see Figure 2).

To sum up, in the case of known parameter, the one-sided ATEWMA TBE scheme is a better alternative to the one-sided AEWMA TBE chart for detecting both upward and downward shifts. On the other hand, irrespective of the known or the estimated parameter case, the one-sided ATEWMA TBE scheme is significantly superior to the one-sided REWMA TBE chart in detecting a shift that is much larger or smaller than the designed shift size τ_R.

6. Real data applications

In this section, two real datasets are employed to illustrate the implementation of the one-sided ATEWM TBE schemes for monitoring mean shifts of high-quality processes. More specifically, one is based on the electronic component failure time monitoring from Samsung company as reported in Qu et al. (2018), and the other one is based on the aircraft reliability monitoring from the Hellenic Air Force (HAF) as reported in Alevizakos & Koukouvinos (2020).

6.1. Failure time monitoring

Samsung company manufactures many kinds of electronic components, including the organic light-emitting diode (OLED). The dataset of OLED failure time using an accelerated life test (ALT) employed here is adapted from Qu et al. (2018), which consists of 30 in-control TBE observations and 20 out-of-control TBE observations, see Table 10.

(Please insert Table 10 here)

As it has been shown in Qu et al. (2018), the failure time X_t under the ALT follows an exponential distribution, and the in-control mean value of the exponential distribution can be estimated from those 30 in-control TBE observations in Table 10 using (10), say,

$$\widehat{\theta}_0 = \frac{1}{30}\sum_{t=1}^{30} X_t \approx 1.27 \text{ min}$$

When the OLED manufacturing process is in-control, we take this estimate as the mean value θ_0 of the OLED failure time under the ALT. In order to ensure the quality of the OLEDs, quality engineers need to pay more attention to the downward shift that occurs in the in-control mean value θ_0, because a decrease in θ_0 means that the quality of OLED deteriorates. On the other hand, since the shift size in the real manufacturing process usually cannot be predicted in advance, it is more realistic to assume that the engineers are interested in detecting both a small downward shift τ_L and a large downward shift τ_S simultaneously, rather than monitoring a particular mean shift level. In this context, the lower-sided ATEWMA TBE scheme can be used to monitor the OLED manufacturing process by checking the time X_t to failure under the ALT.

In this example, the optimal design parameters of the lower-sided ATEWMA TBE scheme can be searched by using the optimal design procedure introduced in Section 4, with the constraint on the desired ARL_0 and the specified shift com-

bination (τ_S, τ_L). More specifically, assuming that $\mathrm{ARL}_0 = 200$, and engineers are interested in detecting both the small downward shift $0.8 \times \theta_0$ and the large downward shift $0.2 \times \theta_0$, i.e., $(\tau_S, \tau_L) = (0.8, 0.2)$. Based on these two settings, the optimal parameter combination $\zeta^* = \{\lambda^*, k^*, H^{-*}\}$ of the proposed scheme is $\{0.1354, 18.2366, 0.6526\}$. Furthermore, three comparative schemes, namely, a lower-sided AEWMA TBE scheme and the other two different lower-sided REWMA TBE schemes (which are respectively designed for $\tau_R = 0.8$ and $\tau_R = 0.2$), are used here to provide a comparison with the lower-sided ATEWMA TBE scheme in monitoring the downward shift of the OLED failure time. Based on $\mathrm{ARL}_0 = 200$, the optimal parameter combination $\{\lambda_A^*, k^*, h_A^{-*}\}$ of the lower-sided AEWMA TBE scheme is $\{0.2545, 11.0204, 0.3453\}$, and the optimal parameter combinations $\{\lambda_R^*, h_R^{-*}\}$ of the lower-sided REWMA TBE schemes for $\tau_R = 0.8$ and $\tau_R = 0.2$ are $\{0.0235, 0.8162\}$ and $\{0.3708, 0.2496\}$, respectively.

With the optimal parameter combinations of these schemes, the charting statistics W_t^- of the lower-sided ATEWMA TBE scheme can be computed using (1), (4), (6), (8), and (9). Meanwhile, the charting statistics $Q_{A,t}^-$ of the lower-sided AEWMA TBE scheme can be obtained using (1), (9), and (41), and the corresponding charting statistics $Q_{R,t}^-$ of the lower-sided REWMA TBE scheme can be given using (1) and (39). All charting statistics are shown in Columns 6 to 9 of Table 10, respectively. It should be noted that, for these lower-sided schemes, an out-of-control signal is generated if the charting statistic falls below the corresponding control limit. For example, when $t = 38$, the charting statistic W_t^- of

the lower-sided ATEWMA TBE scheme falls below its control limit H^{-*}, see Figure 6 (a). This means that an out-of-control signal of the lower-sided ATEWMA TBE scheme is generated and corresponding actions should be taken to identify and remove the downward mean shift. Meanwhile, as we can see from Table 10 and Figures 6 (b), (c), and (d), the lower-sided AEWMA TBE scheme gives an out-of-signal at the 44th TBE observation, the lower-sided REWMA TBE scheme designed for $\tau_R = 0.8$ signals at the 43th TBE observation, and the lower-sided REWMA TBE scheme designed for $\tau_R = 0.2$ signals at the 46th TBE observation. This indicates that, in this example, the lower-sided ATEWMA TBE scheme is superior to both the lower-sided AEWMA TBE scheme and the lower-sided REWMA TBE schemes in monitoring the OLED manufacturing process.

(Please insert Figure 6 here)

6.2. Aircraft reliability monitoring

Another real dataset from the Hellenic Air Force (HAF) as reported in Alevizakos & Koukouvinos (2020) is also employed here to show the implementation of the one-sided ATEWMA TBE scheme. This dataset is related to the accidents of F-16 aircrafts in the HAF. It is worth noting that the time between two accidents of F-16 aircrafts can be regarded as an important quality characteristic concerning aircraft reliability monitoring, as the decrease in the mean value of those time intervals indicates that the reliability of the aircraft declined. In this real dataset, 16 time intervals X_t between successive accidents of F-16 aircrafts are recorded, see Column 2 in Table 11. It has been proved by Alevizakos & Koukouvinos (2020)

that these time intervals X_t between two consecutive accidents of F-16 aircrafts fit an exponential distribution with scale parameter $\theta_1 = 615$ (days). Similar to the assumption in Hu et al. (2021), the in-control value of θ_0 in this example is assumed to be known as 1460 (days). That is to say, the process is acceptable if an accident occurs every four years. Since the investigators are more concerned with a decrease in the mean value of those time intervals X_t, a lower-sided ATEWMA TBE scheme is suggested here to monitor those 16 Phase II TBE observations, where the potential downward shift is $\tau = \theta_1/\theta_0 = 615/1460 = 0.42$.

(Please insert Table 11 here)

Similar to the steps introduced in Alevizakos & Koukouvinos (2020), the design parameters of the scheme should be determined first, imposing the constraint that the acceptable ARL_0 reaches its pre-specified target. In this example, assuming that the investigators decide to set $\mathrm{ARL}_0 = 370$, and the lower-sided ATEWMA TBE scheme designed for $(\tau_s, \tau_L) = (0.7, 0.2)$ can be considered to provide a good protection against the potential downward shift $\tau = 0.42$. With the constraint on $\mathrm{ARL}_0 = 370$, the optimal parameter combination of the proposed scheme is $\{\lambda^*, k^*, H^{-*}\}$=$\{$0.0729,13.5426,0.7412$\}$ (see Table 2). Meanwhile, the lower-sided AEWMA TBE scheme and the other two different lower-sided REWMA TBE schemes (which are respectively designed for $\tau_R = 0.7$ and $\tau_R = 0.2$) are also used here for comparison. Based on $\mathrm{ARL}_0 = 370$, the optimal parameter combination of the lower-sided AEWMA TBE scheme designed for $(\tau_s, \tau_L) = (0.7, 0.2)$ is $\{\lambda_A^*, k^*, h_A^{-*}\}$=$\{$0.2202, 7.9248, 0.3488$\}$ (see Table 5), and the corresponding optimal parameter combinations of the lower-sided

REWMA TBE charts for $\tau_R = 0.7$ and $\tau_R = 0.2$ are $\{\lambda_R^*, h_R^{-*}\}$=$\{0.0362,0.7252\}$ and $\{\lambda_R^*, h_R^{-*}\}$=$\{0.3454,0.2388\}$, respectively (see Table 5).

After determining the optimal parameter combinations, all charting statistics generated by those schemes are recorded in Table 11 and plotted in Figures 7 (a), (b), (c), and (d). As it can be seen that, the lower-sided ATEWMA TBE scheme gives an out-of-control signal at the 16th TBE observation (note that the corresponding 16th charting statistic is bolded in Table 11), while the lower-sided AEWMA TBE scheme and the other two lower-sided REWMA TBE charts cannot detect this downward shift at all. This fact implies that the lower-sided ATEWMA TBE scheme in this example is more effective than the lower-sided AEWMA TBE scheme and the lower-sided REWMA TBE schemes for detecting the downward shift in aircraft reliability monitoring.

(Please insert Figure 7 here)

7. Conclusions

In the manufacturing industry, there are many high-quality processes that can be reasonably modelled using the exponential distribution. In order to monitor such processes, a new one-sided ATEWMA TBE scheme with known and estimated parameters is proposed in this study, for providing a good protection against both small and large shifts assuming a known shift direction. Due to the implementation of Huber's score function, the proposed scheme can be regarded as a smooth combination of a Shewhart TBE chart and a one-sided EWMA TBE chart

using the truncation method. A dedicated Markov chain model is established to evaluate the RL properties of the proposed scheme with known and estimated parameters. Based on the ARL criteria, a two-stage optimal design procedure is developed for searching the optimal parameter combination of the proposed scheme. Numerical results show that, in the case of known parameter, the one-sided ATEWMA TBE scheme performs uniformly better than the other two existing comparative schemes. In addition, the recommended scheme with estimated parameters performs better than the one-sided AEWMA TBE chart in compensating the adverse effect of parameter estimation.

Several research directions are summarized here for future research works. First, a bootstrap-based design approach can be considered to overcome the issue that a large number of Phase I TBE observations are usually unavailable in practice. Secondly, from a practical point of view, both the steady-state and the worst-case scenarios of the recommended scheme are worth studying. Last but not least, the one-sided ATEWMA TBE scheme based on exponential distribution can theoretically be extended to that one based on Gamma distribution for monitoring the sum of inter-arrival times before the rth event.

Disclosure statement

No potential conflict of interest was reported by the author(s).

References

Alevizakos, V., & Koukouvinos, C. (2020). A double exponentially weighted moving average chart for time between events. *Communications in Statistics-Simulation and Computation*, *49*, 2765–2784.

Ali, S., & Pievatolo, A. (2016). High quality process monitoring using a class of inter-arrival time distributions of the renewal process. *Computers & Industrial Engineering*, *94*, 45–62.

Aslam, M., Khan, N., Azam, M., & Jun, C. H. (2014). Designing of a new monitoring t-chart using repetitive sampling. *Information Sciences*, *269*, 210–216.

Capizzi, G., & Masarotto, G. (2003). An adaptive exponentially weighted moving average control chart. *Technometrics*, *45*, 199–207.

Castagliola, P., Tran, K., Celano, G., Rakitzis, A., & Maravelakis, P. (2019). An EWMA-type sign chart with exact run length properties. *Journal of Quality Technology*, *51*, 51–63.

Chiu, J., & Tsai, C. (2013). Properties and performance of one-sided cumulative count of conforming chart with parameter estimation in high-quality processes. *Journal of Applied Statistics*, *40*, 2341–2353.

Chong, N. L., Khoo, M. B., Castagliola, P., Saha, S., & Mim, F. N. (2021). A variable parameters auxiliary information based quality control chart with application in a spring manufacturing process: The markov chain approach. *Quality Engineering*, *33*, 252–270.

Gan, F. (1998). Designs of one-and two-sided exponential ewma charts. *Journal of Quality Technology*, *30*, 55–69.

Haq, A. (2020). One-sided and two one-sided MEWMA charts for monitoring process mean. *Journal of Statistical Computation and Simulation*, *90*, 699–718.

Haq, A., & Khoo, M. B. (2019). New adaptive EWMA control charts for monitoring univariate and multivariate coefficient of variation. *Computers & Industrial Engineering*, *131*, 28–40.

Hu, X., Castagliola, P., Zhong, J., Tang, A., & Qiao, Y. (2021). On the performance of the adaptive ewma chart for monitoring time between events. *Journal of Statistical Computation and Simulation*, *91*, 1175–1211.

Jardim, F. S., Chakraborti, S., & Epprecht, E. K. (2020). Two perspectives for designing a phase II control chart with estimated parameters: The case of the shewhart X chart. *Journal of Quality Technology*, *52*, 198–217.

Mahmoud, M. A., & Maravelakis, P. E. (2010). The performance of the MEWMA control chart when parameters are estimated. *Communications in Statistics-Simulation and Computation*, *39*, 1803–1817.

Mitra, A., Lee, K. B., & Chakraborti, S. (2019). An adaptive exponentially weighted moving average-type control chart to monitor the process mean. *European Journal of Operational Research*, *279*, 902–911.

Montgomery, D. C. (2012). *Introduction to statistical quality control*. (Seventh ed.). New York: John Wiley & Sons.

Ozsan, G., Testik, M. C., & Weiß, C. H. (2010). Properties of the exponential EWMA chart with parameter estimation. *Quality and Reliability Engineering International*, *26*, 555–569.

Perry, M. B. (2020). An EWMA control chart for categorical processes with applications to social network monitoring. *Journal of Quality Technology*, *52*, 182–197.

Psarakis, S. (2015). Adaptive control charts: recent developments and extensions. *Quality and Reliability Engineering International*, *31*, 1265–1280.

Qiao, Y., Sun, J., Castagliola, P., & Hu, X. (2020 in press). Optimal design of one-sided exponential EWMA charts based on median run length and expected median run length. *Communications in Statistics-Theory and Methods*, *0*, 1–21. doi:10.1080/03610926.2020.1782937.

Qu, L., Khoo, M. B. C., Castagliola, P., & He, Z. (2018). Exponential cumulative sums chart for detecting shifts in time-between-events. *International Journal of Production Research*, *56*, 3683–3698.

Saleh, N. A., Mahmoud, M. A., & Abdel-Salam, A. S. G. (2013). The performance of the adaptive exponentially weighted moving average control chart with estimated parameters. *Quality and Reliability Engineering International*, *29*, 595–606.

Santiago, E., & Smith, J. (2013). Control charts based on the exponential distribution: Adapting runs rules for the t chart. *Quality Engineering*, *25*, 85–96.

Sanusi, R. A., Teh, S. Y., & Khoo, M. B. (2020). Simultaneous monitoring of magnitude and time-between-events data with a Max-EWMA control chart. *Computers & Industrial Engineering*, *142*, 106378.

Shu, L., Jiang, W., & Wu, S. (2007). A one-sided ewma control chart for monitoring process means. *Communications in Statistics-Simulation and Computation*, *36*, 901–920.

Tang, A., Castagliola, P., Hu, X., & Sun, J. (2019a). The adaptive EWMA median chart for known and estimated parameters. *Journal of Statistical Computation and Simulation*, *89*, 844–863.

Tang, A., Sun, J., Hu, X., & Castagliola, P. (2019b). A new nonparametric adaptive EWMA control chart with exact run length properties. *Computers & Industrial Engineering*, *130*, 404–419.

Testik, M. C., Kara, O., & Knoth, S. (2020). An algorithmic approach to outlier detection and parameter estimation in Phase I for designing Phase II EWMA control chart. *Computers & Industrial Engineering*, *144*, 106440.

Urbieta, P., Lee HO, L., & Alencar, A. (2017). CUSUM and EWMA control charts for negative binomial distribution. *Quality and Reliability Engineering International*, *33*, 793–801.

Wang, F., Bizuneh, B., & Cheng, X. (2019). One-sided control chart based on support vector machines with differential evolution algorithm. *Quality and Reliability Engineering International*, *35*, 1634–1645.

Wang, H., Sun, H., Li, C., Rahnamayan, S., & Pan, J. (2013). Diversity enhanced particle swarm optimization with neighborhood search. *Information Sciences*, *223*, 119–135.

Xie, F., Castagliola, P., Qiao, Y., Hu, X., & Sun, J. (2021 in press). A one-sided exponentially weighted moving average control chart for time between events. *Journal of Applied Statistics*, *0*, 1–30. doi:10.1080/02664763.2021.1967894.

Xie, Y., Tsui, K., Xie, M., & Goh, T. (2010). Monitoring time-between-events for health management. In *2010 Prognostics and System Health Management Conference* (pp. 1–8). IEEE.

Zhang, C., Xie, M., & Goh, T. N. (2006). Design of exponential control charts using a sequential sampling scheme. *IIE Transactions*, *38*, 1105–1116.

Zhang, M., Megahed, F. M., & Woodall, W. H. (2014). Exponential CUSUM charts with estimated control limits. *Quality and Reliability Engineering International*, *30*, 275–286.

Zwetsloot, I. M., & Woodall, W. H. (2017). A head-to-head comparative study of the conditional performance of control charts based on estimated parameters. *Quality Engineering*, *29*, 244–253.

Appendix A

Similar to the establishment of the Markov chain model for the upper-sided ATEWMA TBE scheme, the in-control region in the downward shift case is denoted as $[H^-, 1/(1-e^{-1})]$, and the transient states are obtained by diving the in-control region into m sub-intervals of the width Δ^-, where

$$\Delta^- = \frac{1}{m}\left(\frac{1}{1-e^{-1}} - H^-\right). \tag{A.1}$$

If we define E_j^- as the mid-point value of the jth sub-interval, say,

$$E_j^- = \frac{1}{1-e^{-1}} - (j - \frac{1}{2})\Delta^-, \tag{A.2}$$

where $j = 1, 2, \ldots, m$. Then, the charting statistic W_t^- in the transient state j can be written as $E_j^- - \Delta^-/2 < W_t^- \leqslant E_j^- + \Delta^-/2$. Furthermore, the transient probabilities $q_{i,j}$ from transient state i to transient state j are computed as follows:

$$\begin{aligned} q_{i,j} &= \Pr\left(W_t^- \in \text{transient state } j \;\middle|\; W_{t-1}^- \in \text{transient state } i\right) \\ &= \Pr\left(E_j^- - E_i^- - \frac{\Delta^-}{2} < \phi(Z_t^- - W_{t-1}^-) \leqslant E_j^- - E_i^- + \frac{\Delta^-}{2}\right) \\ &= \Pr\left(\left(1-e^{-1}\right)\left[E_i^- + \phi^{-1}\left(E_j^- - E_i^- - \frac{\Delta^-}{2}\right)\right] < M_t^- \leqslant \right. \\ &\qquad \left.\left(1-e^{-1}\right)\left[E_i^- + \phi^{-1}\left(E_j^- - E_i^- + \frac{\Delta^-}{2}\right)\right]\right). \end{aligned} \tag{A.3}$$

where $\phi^{-1}(\cdot)$ is defined in (24), $i = 1, 2, \ldots, m$, and $j = 1, 2, \ldots, m$. If we define,

$$\Psi_3 = \left(1 - e^{-1}\right)\left[E_i^- + \phi^{-1}\left(E_j^- - E_i^- - \frac{\Delta^-}{2}\right)\right], \tag{A.4}$$

$$\Psi_4 = \left(1 - e^{-1}\right)\left[E_i^- + \phi^{-1}\left(E_j^- - E_i^- + \frac{\Delta^-}{2}\right)\right], \tag{A.5}$$

the transient probabilities $q_{i,j}$ can be denoted as:

$$q_{i,j} = \begin{cases} 0, & \text{if } \Psi_3 > 1 \\ 1 - F_\Theta\left(\dfrac{\Psi_3}{\tau}\right), & \text{if } \Psi_3 \leqslant 1 \text{ and } \Psi_4 > 1 \\ F_\Theta\left(\dfrac{\Psi_4}{\tau}\right) - F_\Theta\left(\dfrac{\Psi_3}{\tau}\right), & \text{if } \Psi_3 \leqslant 1 \text{ and } \Psi_4 \leqslant 1 \end{cases} \tag{A.6}$$

Additionally, the elements p_j of the initial probability vector $\mathbf{p}$ are given as:

$$p_j = \begin{cases} 1, & E_j^- - \dfrac{\Delta^-}{2} < W_0^- \leqslant E_j^- + \dfrac{\Delta^-}{2} \\ 0, & \text{otherwise} \end{cases} \tag{A.7}$$

where $j = 1, 2, \ldots, m$, and $W_0^- = E(Z_t^-) = 1$. Finally, the ARL value of the lower-sided ATEWMA TBE scheme can be computed using (20).

For the lower-sided ATEWMA TBE scheme with estimated parameters, we define the width of the jth sub-interval as $\widehat{\Delta}^- = \left(1/\left(u - ue^{-\frac{1}{u}}\right) - \widehat{H}^-\right)/m$, and the mid-point value of the jth sub-interval as $\widehat{E}_j^- = 1/\left(u - ue^{-\frac{1}{u}}\right) - (j - 1/2)\widehat{\Delta}^-$. Then, the one-step transient probabilities $\widehat{q}_{i,j}$ in matrix $\widehat{\mathbf{Q}}$ are computed

as follows:

$$\widehat{q}_{i,j} = \begin{cases} 0, & \text{if } \widehat{\Psi}_3 > 1 \\ 1 - F_\Theta\left(\dfrac{\widehat{\Psi}_3}{u \times \tau}\right), & \text{if } \widehat{\Psi}_3 \leqslant 1 \text{ and } \widehat{\Psi}_4 > 1 \\ F_\Theta\left(\dfrac{\widehat{\Psi}_4}{u \times \tau}\right) - F_S\left(\dfrac{\widehat{\Psi}_3}{u \times \tau}\right), & \text{if } \widehat{\Psi}_3 \leqslant 1 \text{ and } \widehat{\Psi}_4 \leqslant 1 \end{cases} \tag{A.8}$$

where

$$\widehat{\Psi}_3 = \left(u - ue^{-\frac{1}{u}}\right)\left[\widehat{E}_i^- + \phi^{-1}\left(\widehat{E}_j^- - \widehat{E}_i^- - \frac{\widehat{\Delta}^-}{2}\right)\right], \tag{A.9}$$

$$\widehat{\Psi}_4 = \left(u - ue^{-\frac{1}{u}}\right)\left[\widehat{E}_i^- + \phi^{-1}\left(\widehat{E}_j^- - \widehat{E}_i^- + \frac{\widehat{\Delta}^-}{2}\right)\right], \tag{A.10}$$

and $i = 1, 2, \ldots, m$, $j = 1, 2, \ldots, m$. In addition, the elements $\widehat{p}_j$ of the initial probability vector $\widehat{\mathbf{p}}$ are given as,

$$\widehat{p}_j = \begin{cases} 1, & \widehat{E}_j^- - \dfrac{\widehat{\Delta}^-}{2} < \widehat{W}_0^- \leqslant \widehat{E}_j^- + \dfrac{\widehat{\Delta}^-}{2} \\ 0, & \text{otherwise} \end{cases} \tag{A.11}$$

where $\widehat{W}_0^- = E(\widehat{Z}_t^-) = 1$. After determining the matrix $\widehat{\mathbf{Q}}$ and the vector $\widehat{\mathbf{p}}$, the ARL value of the lower-sided ATEWMA TBE scheme with estimated parameters are computed using (29) and (30).

Table 1: Optimal parameter combinations ζ^* of the upper-sided ATEWMA TBE scheme for $\mathrm{ARL}_0 \in \{200, 370, 500\}$.

τ_S	τ_L	$\mathrm{ARL}_0 = 200$			$\mathrm{ARL}_0 = 370$			$\mathrm{ARL}_0 = 500$		
		λ^*	k^*	H^{+*}	λ^*	k^*	H^{+*}	λ^*	k^*	H^{+*}
1.1	3	0.1883	10.0043	1.6032	0.1857	14.9105	1.6990	0.0710	5.0794	1.3378
1.3	3	0.1414	4.7324	1.4687	0.2051	4.9170	1.7620	0.0891	13.8196	1.4046
1.5	3	0.0997	19.3077	1.3443	0.1167	13.8295	1.4705	0.1013	18.1002	1.4495
1.1	4	0.1972	18.7462	1.6286	0.2286	14.6487	1.8375	0.2941	6.8258	2.1175
1.3	4	0.3070	3.6431	1.9368	0.1585	10.9228	1.6104	0.1508	7.0995	1.6268
1.5	4	0.3698	19.5277	2.1067	0.1216	8.6812	1.4872	0.1874	7.2428	1.7544
1.1	5	0.1284	6.9732	1.4307	0.1865	4.1443	1.7107	0.1213	10.2955	1.5227
1.3	5	0.1896	9.5962	1.6068	0.1671	13.9985	1.6391	0.2758	13.3147	2.0555
1.5	5	0.1655	19.3518	1.5380	0.3105	7.0272	2.0981	0.1347	7.0693	1.5702

Table 2: Optimal parameter combinations ζ^* of the lower-sided ATEWMA TBE scheme for $\mathrm{ARL}_0 \in \{200, 370, 500\}$.

τ_S	τ_L	$\mathrm{ARL}_0 = 200$			$\mathrm{ARL}_0 = 370$			$\mathrm{ARL}_0 = 500$		
		λ^*	k^*	H^{-*}	λ^*	k^*	H^{-*}	λ^*	k^*	H^{-*}
0.9	0.3	0.1411	8.9318	0.6428	0.1124	14.4142	0.6561	0.1127	4.5151	0.6388
0.8	0.3	0.0687	15.2093	0.7845	0.0700	13.9071	0.7478	0.1103	2.8205	0.6437
0.7	0.3	0.1417	13.6767	0.6420	0.0713	18.4310	0.7450	0.0741	5.3099	0.7228
0.9	0.2	0.1848	6.1138	0.5754	0.1820	13.2921	0.5387	0.1534	13.8204	0.5655
0.8	0.2	0.1354	18.2366	0.6526	0.1422	10.5375	0.6017	0.1787	17.9492	0.5258
0.7	0.2	0.2623	2.1815	0.4754	0.0729	13.5426	0.7412	0.1381	2.1017	0.5917
0.9	0.1	0.2833	16.5755	0.4517	0.2788	12.4893	0.4157	0.2669	12.2793	0.4111
0.8	0.1	0.2552	7.4753	0.4837	0.3418	6.6908	0.3520	0.2784	17.8617	0.3984
0.7	0.1	0.2997	12.6632	0.4341	0.2951	2.3076	0.3983	0.2216	16.6469	0.4660

Table 3: In-control ARL comparisons of the upper-sided and lower-sided ATEWMA TBE schemes for $\ell \in \{20, 50, 100, 300, 500, 1000, +\infty\}$.

τ_S	τ_L	ℓ						
		20	50	100	300	500	1000	$+\infty$
1.1	3	518.55	415.28	390.90	376.62	373.86	371.92	370.00
1.3	3	516.66	414.89	390.81	376.63	373.98	371.97	370.00
1.5	3	526.28	416.00	391.09	376.68	373.85	371.87	370.00
1.1	4	513.36	414.25	390.57	376.56	373.88	371.92	370.00
1.3	4	522.67	416.01	391.35	376.81	374.10	372.09	369.99
1.5	4	525.68	415.93	391.06	376.54	373.86	371.91	370.00
1.1	5	529.28	417.98	392.16	377.03	374.21	372.06	370.00
1.3	5	521.32	415.72	391.17	376.71	373.94	371.97	370.00
1.5	5	504.58	412.34	389.77	376.32	373.74	371.85	370.00
0.9	0.3	452.39	397.87	383.04	373.97	372.11	370.90	370.00
0.8	0.3	444.44	395.99	382.92	374.12	372.79	371.52	370.00
0.7	0.3	443.67	395.41	381.92	373.87	372.21	370.66	370.00
0.9	0.2	453.93	398.98	383.96	374.52	372.64	371.36	370.00
0.8	0.2	454.02	398.68	383.69	374.26	372.42	371.16	369.99
0.7	0.2	444.18	395.58	381.91	373.38	371.82	371.00	370.00
0.9	0.1	447.93	397.42	383.11	374.40	372.64	371.36	370.00
0.8	0.1	442.56	395.60	382.24	373.88	372.21	371.03	370.00
0.7	0.1	446.62	396.97	383.13	374.26	372.57	371.33	370.00

Table 4: The adjusted control limits $\widehat{H}^{+*}$ and $\widehat{H}^{-*}$ of the upper-sided and lower-sided ATEWMA TBE schemes for $\ell \in \{20, 50, 100, 300, 500, 1000\}$.

τ_S	τ_L	ℓ					
		20	50	100	300	500	1000
1.1	3	1.6504	1.6809	1.6902	1.6961	1.6973	1.6982
1.3	3	1.7098	1.7425	1.7524	1.7589	1.7601	1.7611
1.5	3	1.4350	1.4574	1.4641	1.4684	1.4693	1.4699
1.1	4	1.7815	1.8165	1.8272	1.8341	1.8355	1.8365
1.3	4	1.5665	1.5940	1.6024	1.6077	1.6088	1.6096
1.5	4	1.4508	1.4737	1.4807	1.4851	1.4860	1.4866
1.1	5	1.6551	1.6891	1.7000	1.7072	1.7086	1.7097
1.3	5	1.5937	1.6221	1.6308	1.6364	1.6375	1.6383
1.5	5	2.0291	2.0722	2.0854	2.0939	2.0956	2.0968
0.9	0.3	0.6667	0.6602	0.6580	0.6567	0.6564	0.6562
0.8	0.3	0.7564	0.7511	0.7495	0.7483	0.7481	0.7480
0.7	0.3	0.7537	0.7484	0.7466	0.7455	0.7453	0.7451
0.9	0.2	0.5506	0.5433	0.5409	0.5395	0.5391	0.5389
0.8	0.2	0.6131	0.6060	0.6038	0.6023	0.6021	0.6019
0.7	0.2	0.7499	0.7445	0.7428	0.7416	0.7414	0.7413
0.9	0.1	0.4270	0.4200	0.4178	0.4164	0.4161	0.4159
0.8	0.1	0.3623	0.3560	0.3539	0.3527	0.3524	0.3522
0.7	0.1	0.4093	0.4025	0.4003	0.3989	0.3987	0.3985

Table 5: Optimal parameter combinations of the one-sided AEWMA TBE scheme and the one-sided REWMA TBE scheme in both the known ($\ell = +\infty$) and the estimated ($\ell = 100$) parameter cases for in-control $\mathrm{ARL} = 370$.

AEWMA						REWMA			
				$\ell = +\infty$	$\ell = 100$			$\ell = +\infty$	$\ell = 100$
τ_S	τ_L	λ_A^*	k^*	h_A^{+*}	$\widehat{h}_A^{+*}$	τ_R	λ_R^*	h_R^{+*}	$\widehat{h}_R^{+*}$
1.1	3	0.1925	12.2082	2.2150	2.0742	1.1	0.0070	1.0973	1.0721
1.3	3	0.2459	7.9165	2.4726	2.3280	1.3	0.0233	1.2510	1.2086
1.5	3	0.0931	6.9417	1.7027	1.5652	1.5	0.0430	1.3962	1.3462
1.1	4	0.1802	5.0758	2.2261	2.0794	1.7	0.0636	1.5288	1.4740
1.3	4	0.2638	6.3455	2.5572	2.4112	2	0.0945	1.7087	1.6487
1.5	4	0.2839	10.3390	2.6514	2.5033	2.5	0.1435	1.9699	1.9033
1.1	5	0.1725	5.3827	2.1560	2.0147	3	0.1884	2.1951	2.1230
1.3	5	0.3131	13.2758	2.7879	2.6369	4	0.2666	2.5711	2.4898
1.5	5	0.2524	5.1444	2.5603	2.4029	5	0.3328	2.8795	2.7907
τ_S	τ_L	λ_A^*	k^*	h_A^{-*}	$\widehat{h}_A^{-*}$	τ_R	λ_R^*	h_R^{-*}	$\widehat{h}_R^{-*}$
0.9	0.3	0.1541	2.4721	0.4347	0.4538	0.9	0.0071	0.9080	0.9291
0.8	0.3	0.1506	9.3503	0.4400	0.4594	0.8	0.0187	0.8168	0.8434
0.7	0.3	0.1436	15.0109	0.4512	0.4716	0.7	0.0362	0.7252	0.7506
0.9	0.2	0.2171	15.9662	0.3522	0.3648	0.6	0.0613	0.6331	0.6547
0.8	0.2	0.2300	5.5258	0.3381	0.3498	0.5	0.0970	0.5394	0.5567
0.7	0.2	0.2202	7.9248	0.3488	0.3611	0.4	0.1484	0.4434	0.4565
0.9	0.1	0.3396	0.5974	0.2219	0.2241	0.3	0.2243	0.3442	0.3533
0.8	0.1	0.3830	10.3640	0.2139	0.2192	0.2	0.3454	0.2388	0.2443
0.7	0.1	0.3852	16.0606	0.2125	0.2178	0.1	0.5628	0.1248	0.1271

Table 6: ARL_1 values of the upper-sided ATEWMA TBE scheme and the upper-sided AEWMA TBE scheme in detecting upward shifts τ ($\mathrm{ARL}_0 = 370$).

τ_S	τ_L	Schemes	τ									
			1.1	1.3	1.5	1.7	2	2.5	3	3.5	4	5
1.1	3	AEWMA	182.06	65.37	33.13	20.65	12.73	7.73	5.66	4.55	3.86	3.06
		ATEWMA	176.06	61.83	31.32	19.60	12.12	7.37	5.39	4.32	3.67	2.91
1.3	3	AEWMA	188.05	69.53	35.33	21.85	13.25	7.88	5.69	4.54	3.83	3.02
		ATEWMA	178.89	63.56	32.18	20.04	12.31	7.42	5.40	4.32	3.66	2.90
1.5	3	AEWMA	165.49	55.88	28.87	18.70	12.13	7.77	5.83	4.75	4.06	3.24
		ATEWMA	162.97	54.68	28.03	17.95	11.46	7.20	5.35	4.34	3.70	2.95
1.1	4	AEWMA	189.54	69.67	35.16	21.71	13.20	7.89	5.70	4.54	3.83	3.01
		ATEWMA	182.04	65.61	33.24	20.62	12.58	7.52	5.44	4.34	3.67	2.90
1.3	4	AEWMA	189.76	70.79	36.02	22.24	13.44	7.94	5.71	4.54	3.83	3.01
		ATEWMA	171.47	59.12	29.99	18.89	11.80	7.26	5.34	4.30	3.66	2.91
1.5	4	AEWMA	191.53	72.13	36.78	22.68	13.65	8.02	5.74	4.55	3.83	3.01
		ATEWMA	164.15	55.27	28.29	18.08	11.50	7.21	5.35	4.34	3.70	2.95
1.1	5	AEWMA	184.87	66.70	33.68	20.93	12.85	7.77	5.66	4.53	3.83	3.02
		ATEWMA	178.86	63.28	32.00	19.96	12.30	7.45	5.43	4.36	3.69	2.92
1.3	5	AEWMA	193.88	73.95	37.83	23.30	13.95	8.13	5.79	4.57	3.84	3.00
		ATEWMA	173.01	60.01	30.43	19.13	11.91	7.30	5.36	4.32	3.67	2.91
1.5	5	AEWMA	193.95	73.46	37.36	22.96	13.77	8.06	5.75	4.55	3.82	2.99
		ATEWMA	190.69	71.70	36.57	22.53	13.51	7.88	5.61	4.43	3.71	2.91

Table 7: ARL_1 values of the lower-sided ATEWMA TBE scheme and the lower-sided AEWMA TBE scheme in detecting downward shifts τ ($\mathrm{ARL}_0 = 370$).

τ_S	τ_L	Schemes	τ									
			0.95	0.9	0.8	0.7	0.6	0.5	0.4	0.3	0.2	0.1
0.9	0.3	AEWMA	270.40	197.00	104.62	56.86	32.63	20.29	13.77	10.10	7.87	6.41
		ATEWMA	265.76	191.48	101.14	55.45	32.03	19.67	12.84	8.86	6.45	4.97
0.8	0.3	AEWMA	269.70	196.02	103.74	56.32	32.38	20.21	13.77	10.13	7.92	6.45
		ATEWMA	253.14	175.58	88.91	48.77	29.09	18.70	12.79	9.19	6.89	5.41
0.7	0.3	AEWMA	268.31	194.12	102.05	55.30	31.90	20.05	13.77	10.21	8.02	6.56
		ATEWMA	253.77	176.36	89.51	49.14	29.29	18.82	12.86	9.23	6.92	5.43
0.9	0.2	AEWMA	280.62	211.55	118.61	66.17	37.57	22.34	14.24	9.82	7.28	5.70
		ATEWMA	278.97	209.62	117.62	66.02	37.59	22.06	13.55	8.79	6.06	4.47
0.8	0.2	AEWMA	282.39	214.14	121.29	68.08	38.68	22.86	14.42	9.82	7.19	5.59
		ATEWMA	272.19	200.12	108.65	60.05	34.33	20.58	13.05	8.77	6.23	4.68
0.7	0.2	AEWMA	281.06	212.18	119.26	66.63	37.84	22.46	14.28	9.82	7.25	5.67
		ATEWMA	254.28	176.97	89.92	49.30	29.31	18.77	12.79	9.16	6.85	5.38
0.9	0.1	AEWMA	306.41	249.78	161.22	99.88	59.38	34.09	19.24	11.02	6.66	4.29
		ATEWMA	291.03	227.48	136.47	80.12	46.32	26.68	15.57	9.41	6.03	4.19
0.8	0.1	AEWMA	298.41	238.78	149.23	90.37	53.25	30.88	17.99	10.84	6.94	4.80
		ATEWMA	296.86	236.53	146.97	88.76	52.22	30.14	17.29	10.08	6.15	4.04
0.7	0.1	AEWMA	298.59	239.07	149.59	90.68	53.47	31.02	18.06	10.86	6.95	4.79
		ATEWMA	292.63	229.94	139.26	82.36	47.82	27.53	15.98	9.56	6.04	4.14

Table 8: $\widehat{\mathrm{ARL}}_1$ values of the upper-sided ATEWMA TBE scheme and the upper-sided AEWMA TBE scheme in detecting upward shifts τ ($\widehat{\mathrm{ARL}}_0 = 370$, $\ell = 100$).

τ_S	τ_L	Schemes	τ									
			1.1	1.3	1.5	1.7	2	2.5	3	3.5	4	5
1.1	3	AEWMA	170.42	57.83	28.96	18.11	11.28	6.97	5.16	4.18	3.57	2.86
		ATEWMA	175.51	61.38	31.04	19.40	11.99	7.29	5.33	4.28	3.64	2.88
1.3	3	AEWMA	178.82	63.10	31.65	19.58	11.96	7.21	5.26	4.23	3.59	2.86
		ATEWMA	178.40	63.18	31.94	19.89	12.22	7.37	5.37	4.30	3.64	2.88
1.5	3	AEWMA	144.14	44.34	22.88	15.05	9.98	6.56	5.02	4.14	3.58	2.90
		ATEWMA	162.41	54.27	27.78	17.78	11.34	7.13	5.31	4.30	3.67	2.93
1.1	4	AEWMA	180.78	63.13	31.36	19.37	11.89	7.23	5.30	4.27	3.63	2.88
		ATEWMA	181.51	65.18	32.96	20.44	12.47	7.46	5.40	4.31	3.64	2.88
1.3	4	AEWMA	181.16	64.66	32.48	20.05	12.19	7.30	5.30	4.24	3.60	2.86
		ATEWMA	170.98	58.75	29.77	18.75	11.72	7.21	5.31	4.28	3.64	2.90
1.5	4	AEWMA	183.42	66.24	33.35	20.54	12.43	7.39	5.34	4.27	3.61	2.86
		ATEWMA	163.55	54.82	28.01	17.88	11.38	7.13	5.30	4.30	3.67	2.93
1.1	5	AEWMA	175.25	59.84	29.78	18.53	11.51	7.08	5.23	4.23	3.61	2.88
		ATEWMA	177.87	62.62	31.62	19.73	12.16	7.38	5.39	4.32	3.67	2.90
1.3	5	AEWMA	186.43	68.41	34.56	21.25	12.78	7.53	5.41	4.30	3.63	2.86
		ATEWMA	172.50	59.62	30.19	18.96	11.81	7.24	5.32	4.28	3.64	2.89
1.5	5	AEWMA	186.10	67.47	33.83	20.77	12.54	7.45	5.38	4.30	3.63	2.87
		ATEWMA	190.19	71.28	36.30	22.35	13.40	7.82	5.57	4.40	3.69	2.89

Table 9: $\widehat{\mathrm{ARL}}_1$ values of the lower-sided ATEWMA TBE scheme and the lower-sided AEWMA TBE scheme in detecting downward shifts τ ($\widehat{\mathrm{ARL}}_0 = 370$, $\ell = 100$).

τ_S	τ_L	Schemes	τ									
			0.95	0.9	0.8	0.7	0.6	0.5	0.4	0.3	0.2	0.1
0.9	0.3	AEWMA	265.38	190.06	98.17	52.45	29.93	18.66	12.75	9.43	7.39	6.08
		ATEWMA	266.16	191.98	101.51	55.62	32.07	19.64	12.78	8.80	6.39	4.90
0.8	0.3	AEWMA	264.44	188.79	97.08	51.80	29.62	18.55	12.74	9.45	7.43	6.12
		ATEWMA	253.66	176.22	89.39	49.05	29.23	18.78	12.82	9.20	6.88	5.40
0.7	0.3	AEWMA	262.65	186.41	95.06	50.61	29.05	18.34	12.70	9.48	7.50	6.20
		ATEWMA	254.15	176.80	89.77	49.21	29.27	18.75	12.78	9.15	6.85	5.37
0.9	0.2	AEWMA	277.66	207.23	114.16	62.85	35.43	21.05	13.47	9.34	6.96	5.51
		ATEWMA	279.39	210.22	118.20	66.42	37.81	22.17	13.59	8.80	6.06	4.46
0.8	0.2	AEWMA	279.69	210.17	117.13	64.94	36.63	21.61	13.67	9.37	6.91	5.42
		ATEWMA	272.63	200.72	109.17	60.37	34.49	20.65	13.07	8.76	6.22	4.66
0.7	0.2	AEWMA	278.16	207.96	114.89	63.36	35.72	21.18	13.52	9.35	6.95	5.48
		ATEWMA	254.71	177.48	90.27	49.47	29.37	18.78	12.77	9.13	6.82	5.36
0.9	0.1	AEWMA	304.93	249.03	161.27	100.15	59.60	34.19	19.23	10.97	6.60	4.24
		ATEWMA	291.38	228.01	137.05	80.57	46.60	26.82	15.63	9.42	6.02	4.17
0.8	0.1	AEWMA	297.28	236.99	147.06	88.48	51.86	29.97	17.44	10.53	6.77	4.73
		ATEWMA	297.18	237.02	147.55	89.23	52.54	30.31	17.37	10.10	6.15	4.02
0.7	0.1	AEWMA	297.48	237.30	147.44	88.80	52.09	30.11	17.52	10.56	6.78	4.72
		ATEWMA	292.97	230.46	139.85	82.82	48.11	27.68	16.04	9.57	6.04	4.12

Table 10: The OLED failure time X_t and the charting statistics corresponding to the lower-sided ATEWMA TBE, the lower-sided AEWMA TBE, and the lower-sided REWMA TBE schemes.

t	X_t (mins)	M_t	ATEWMA			AEWMA	REWMA ($\tau_R = 0.8$)	REWMA ($\tau_R = 0.2$)
			M_t^-	Z_t^-	W_t^-	$Q_{A,t}^-$	$Q_{R,t}^-$	$Q_{R,t}^-$
1.	1.07	0.8425	0.8425	1.3328	1.0451	0.9599	0.9963	0.9416
2.	0.54	0.4252	0.4252	0.6727	0.9946	0.8238	0.9829	0.7501
3.	0.54	0.4252	0.4252	0.6727	0.9510	0.7224	0.9698	0.6296
4.	0.72	0.5669	0.5669	0.8969	0.9437	0.6828	0.9603	0.6064
5.	2.53	1.9921	1	1.5820	1.0301	1	0.9846	1
6.	1.26	0.9921	0.9921	1.5695	1.1032	0.9980	0.9847	0.9971
7.	0.48	0.3780	0.3780	0.5979	1.0348	0.8402	0.9705	0.7675
8.	1.78	1.4016	1	1.5820	1.1088	0.9831	0.9806	1
9.	1.26	0.9921	0.9921	1.5695	1.1712	0.9854	0.9809	0.9971
10.	2.27	1.7874	1	1.5820	1.2268	1	0.9998	1
11.	2.19	1.7244	1	1.5820	1.2749	1	1	1
12.	1.10	0.8661	0.8661	1.3702	1.2878	0.9659	0.9969	0.9504
13.	0.60	0.4724	0.4724	0.7474	1.2147	0.8403	0.9845	0.7732
14.	0.97	0.7638	0.7638	1.2083	1.2138	0.8209	0.9793	0.7697
15.	3.16	2.4882	1	1.5820	1.2636	1	1	1
16.	2.93	2.3071	1	1.5820	1.3067	1	1	1
17.	0.99	0.7795	0.7795	1.2332	1.2968	0.9439	0.9948	0.9182
18.	1.28	1.0079	1	1.5820	1.3354	0.9602	0.9951	0.9515
19.	0.12	0.0945	0.0945	0.1495	1.1748	0.7399	0.9740	0.6337
20.	0.19	0.1496	0.1496	0.2367	1.0478	0.5896	0.9546	0.4542
21.	0.94	0.7402	0.7402	1.1709	1.0645	0.6279	0.9495	0.5602
22.	1.08	0.8504	0.8504	1.3453	1.1025	0.6846	0.9472	0.6678
23.	2.31	1.8189	1	1.5820	1.1674	0.9732	0.9677	1
24.	3.11	2.4488	1	1.5820	1.2235	1	1	1
25.	0.28	0.2205	0.2205	0.3488	1.1051	0.8016	0.9817	0.7110
26.	0.66	0.5197	0.5197	0.8221	1.0668	0.7299	0.9708	0.6400
27.	0.68	0.5354	0.5354	0.8470	1.0370	0.6804	0.9606	0.6012
28.	0.75	0.5906	0.5906	0.9342	1.0231	0.6575	0.9519	0.5973
29.	0.47	0.3701	0.3701	0.5855	0.9639	0.5844	0.9382	0.5130
30.	1.82	1.4331	1	1.5820	1.0476	0.8004	0.9499	0.8542
31.	0.06	0.0472	0.0472	0.0747	0.9158	0.6087	0.9286	0.5550
32.	0.44	0.3465	0.3465	0.5481	0.8660	0.5420	0.9150	0.4777
33.	0.21	0.1654	0.1654	0.2616	0.7842	0.4461	0.8973	0.3619
34.	0.25	0.1969	0.1969	0.3114	0.7202	0.3827	0.8809	0.3007
35.	1.75	1.3780	1	1.5820	0.8369	0.6360	0.8926	0.7001
36.	0.07	0.0551	0.0551	0.0872	0.7354	0.4881	0.8729	0.4610
37.	0.36	0.2835	0.2835	0.4484	0.6965	0.4361	0.8590	0.3951
38.	0.28	0.2205	0.2205	0.3488	**0.6494**	0.3812	0.8440	0.3304
39.	1.43	1.1260	1	1.5820	0.7757	0.5707	0.8507	0.6254
40.	0.31	0.2441	0.2441	0.3862	0.7230	0.4876	0.8364	0.4840
41.	0.86	0.6772	0.6772	1.0713	0.7701	0.5359	0.8327	0.5556
42.	0.17	0.1339	0.1339	0.2118	0.6945	0.4335	0.8162	0.3992
43.	0.29	0.2283	0.2283	0.3612	0.6494	0.3813	**0.8024**	0.3359
44.	0.30	0.2362	0.2362	0.3737	0.6121	**0.3444**	0.7891	0.2989
45.	0.29	0.2283	0.2283	0.3612	0.5781	0.3149	0.7759	0.2728
46.	0.22	0.1732	0.1732	0.2740	0.5369	0.2788	0.7618	**0.2358**
47.	0.04	0.0315	0.0315	0.0498	0.4710	0.2159	0.7446	0.1601
48.	0.47	0.3701	0.3701	0.5855	0.4865	0.2551	0.7358	0.2379
49.	0.23	0.1811	0.1811	0.2865	0.4594	0.2363	0.7228	0.2169
50.	0.44	0.3465	0.3465	0.5481	0.4714	0.2643	0.7139	0.2649

Table 11: The time X_t between consecutive F-16 accidents and the corresponding charting statistics of the lower-sided ATEWMA TBE, the lower-sided AEWMA TBE, and the lower-sided REWMA TBE schemes.

t	X_t (days)	M_t	ATEWMA			AEWMA	REWMA ($\tau_R = 0.7$)	REWMA ($\tau_R = 0.2$)
			M_t^-	Z_t^-	W_t^-	$Q_{A,t}^-$	$Q_{R,t}^-$	$Q_{R,t}^-$
1.	1456	0.9973	0.9973	1.5776	1.0421	0.9994	0.9999	0.9991
2.	231	0.1582	0.1582	0.2503	0.9844	0.8142	0.9694	0.7086
3.	691	0.4733	0.4733	0.7487	0.9672	0.7391	0.9515	0.6273
4.	122	0.0836	0.0836	0.1322	0.9063	0.5948	0.9201	0.4395
5.	718	0.4918	0.4918	0.7780	0.8970	0.5721	0.9045	0.4576
6.	1147	0.7856	0.7856	1.2428	0.9222	0.6191	0.9002	0.5709
7.	225	0.1541	0.1541	0.2438	0.8727	0.5167	0.8732	0.4269
8.	706	0.4836	0.4836	0.7650	0.8649	0.5094	0.8591	0.4465
9.	499	0.3418	0.3418	0.5407	0.8412	0.4725	0.8404	0.4103
10.	587	0.4021	0.4021	0.6360	0.8263	0.4570	0.8245	0.4075
11.	561	0.3842	0.3842	0.6079	0.8104	0.4410	0.8086	0.3994
12.	547	0.3747	0.3747	0.5927	0.7945	0.4264	0.7929	0.3909
13.	448	0.3068	0.3068	0.4854	0.7720	0.4000	0.7753	0.3619
14.	1561	1.0692	1	1.5820	0.8310	0.5474	0.7859	0.6062
15.	53	0.0363	0.0363	0.0574	0.7746	0.4348	0.7588	0.4093
16.	280	0.1918	0.1918	0.3034	**0.7403**	0.3813	0.7383	0.3342

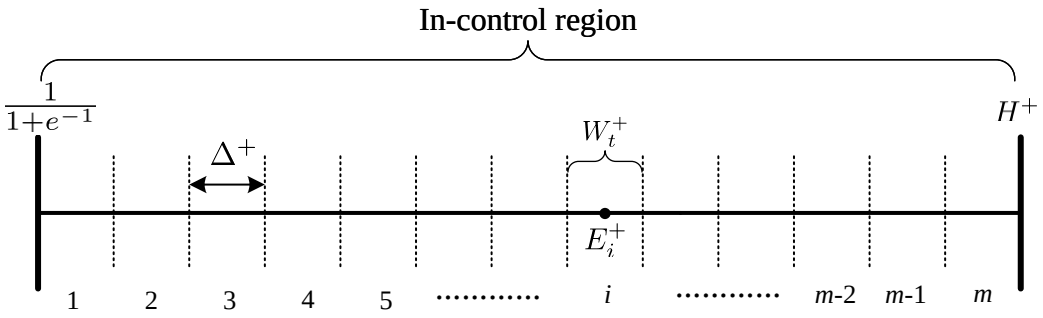

Figure 1: The Markov chain model of the upper-sided ATEWMA TBE scheme.

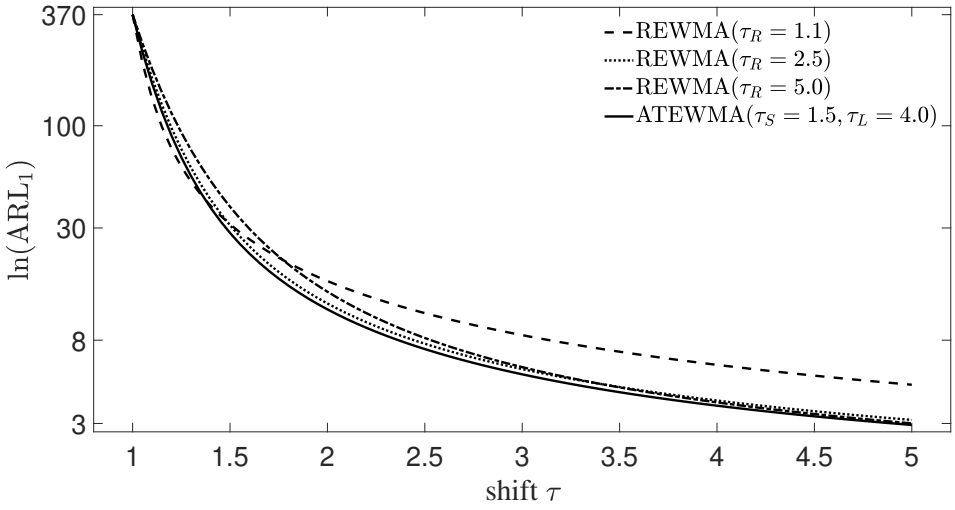

Figure 2: $\ln(\mathrm{ARL}_1)$ comparisons among the upper-sided ATEWMA TBE scheme and three different upper-sided REWMA TBE schemes in detecting upward shifts τ ($\mathrm{ARL}_0 = 370$).

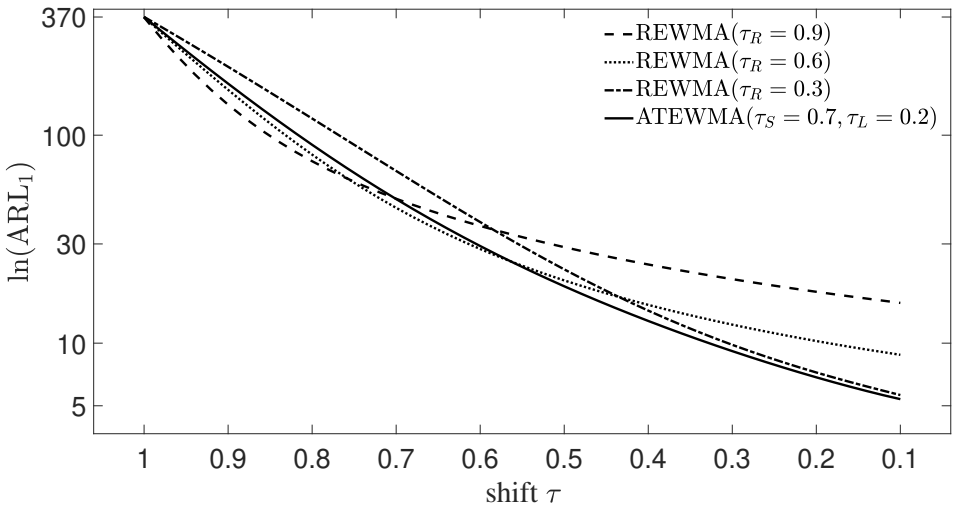

Figure 3: $\ln(\mathrm{ARL}_1)$ comparisons among the lower-sided ATEWMA TBE scheme and three different lower-sided REWMA TBE schemes in detecting downward shifts τ ($\mathrm{ARL}_0 = 370$).

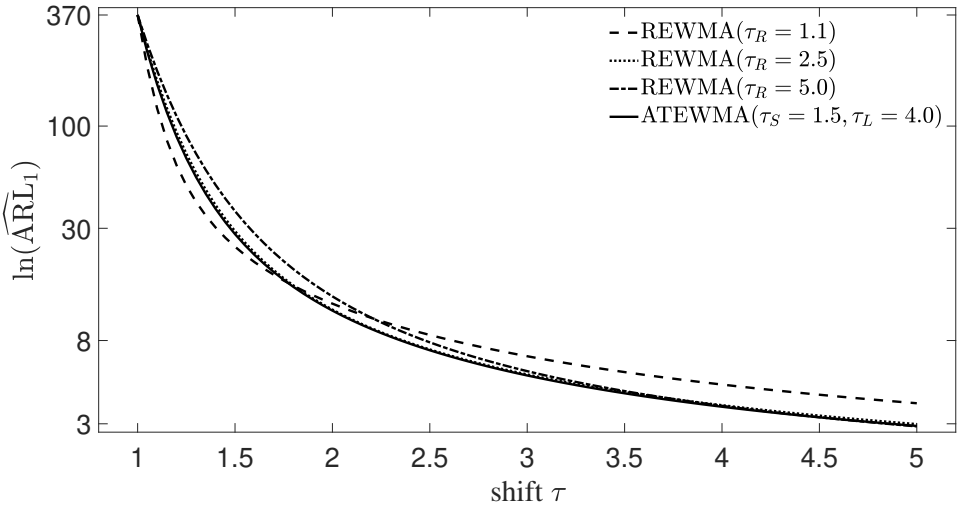

Figure 4: $\ln(\widehat{\mathrm{ARL}}_1)$ comparisons among the upper-sided ATEWMA TBE scheme and three different upper-sided REWMA TBE schemes in detecting upward shifts τ ($\mathrm{ARL}_0 = 370$, $\ell = 100$).

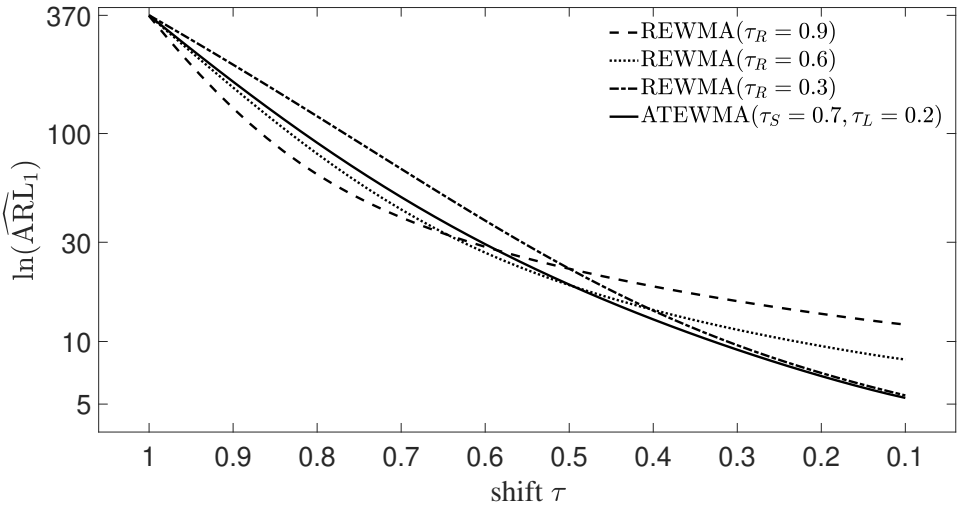

Figure 5: $\ln(\widehat{\mathrm{ARL}}_1)$ comparisons among the lower-sided ATEWMA TBE scheme and three different lower-sided REWMA TBE schemes in detecting downward shifts τ ($\mathrm{ARL}_0 = 370$, $\ell = 100$).

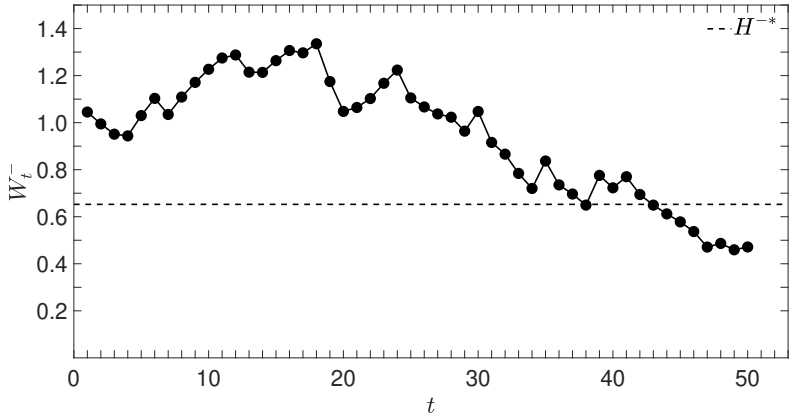

(a) The lower-sided ATEWMA TBE scheme

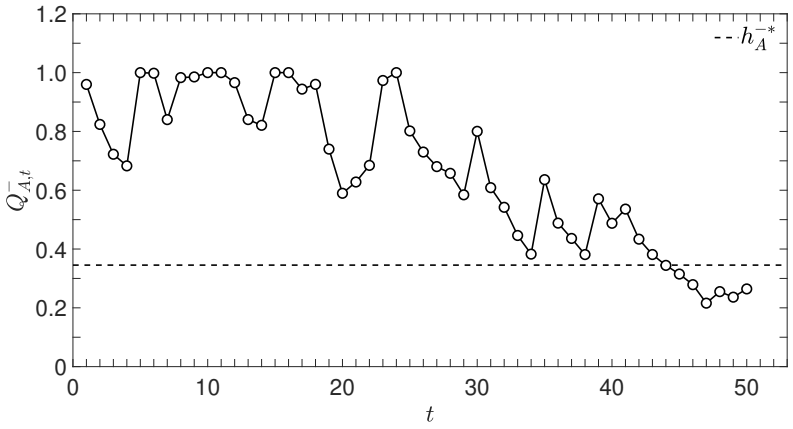

(b) The lower-sided AEWMA TBE scheme

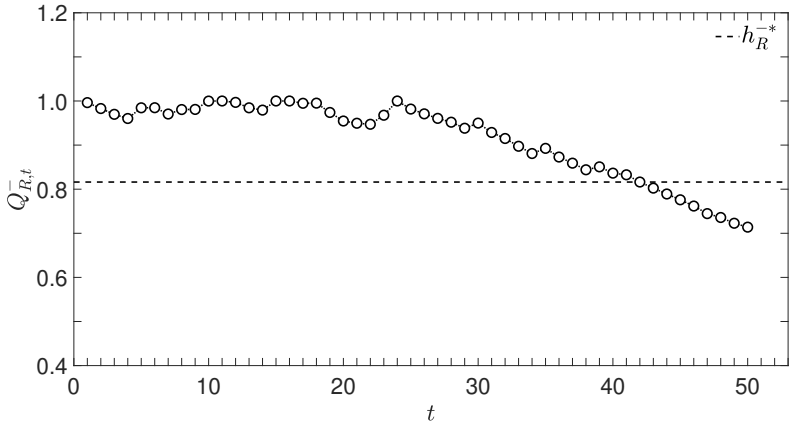

(c) The lower-sided REWMA TBE scheme designed for $\tau_R = 0.8$

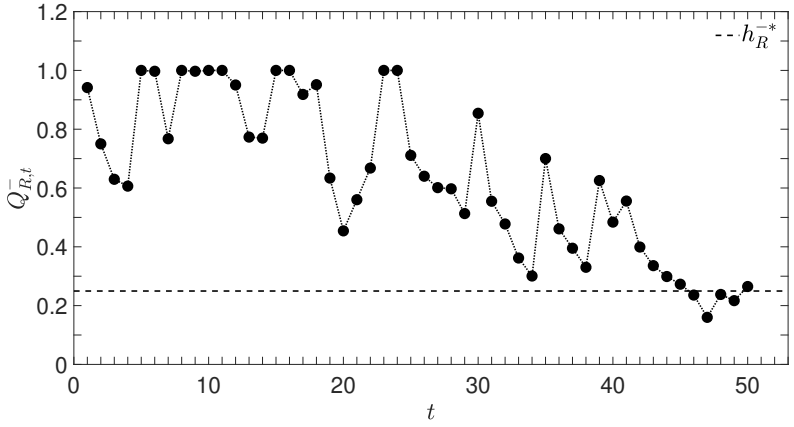

(d) The lower-sided REWMA TBE scheme designed for $\tau_R = 0.2$

Figure 6: The OLED failure time monitoring presented in Table 10.

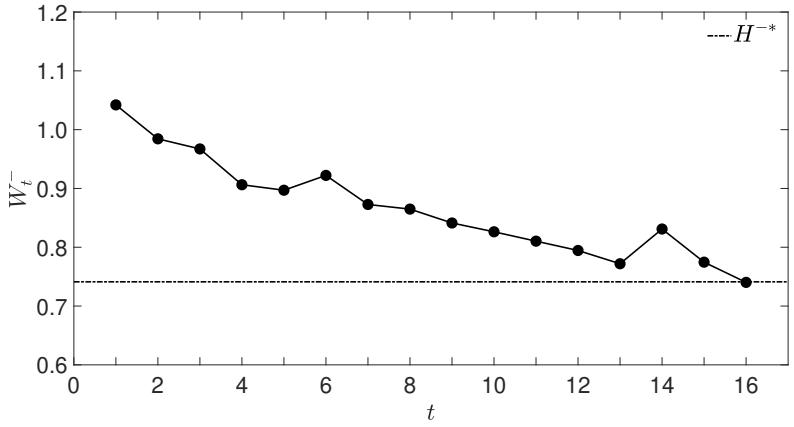

(a) The lower-sided ATEWMA TBE scheme

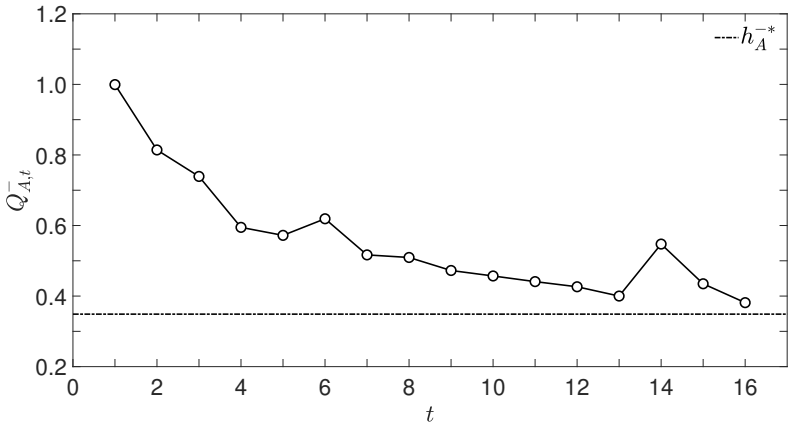

(b) The lower-sided AEWMA TBE scheme

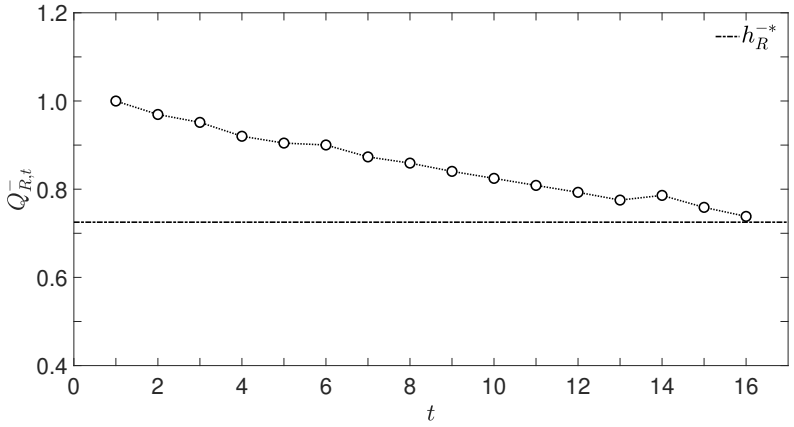

(c) The lower-sided REWMA TBE scheme designed for $\tau_R = 0.7$

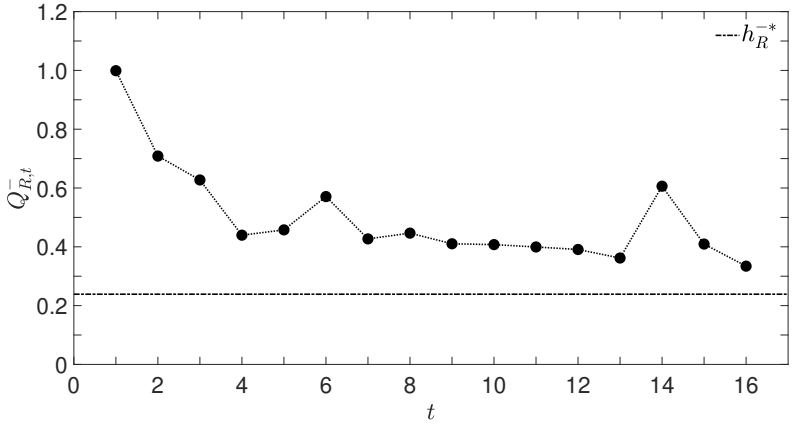

(d) The lower-sided REWMA TBE scheme designed for $\tau_R = 0.2$

Figure 7: The aircraft accident monitoring shown in Table 11.